Elsevier Editorial System(tm) for Clinical Nutrition

Manuscript Draft

Manuscript Number:

Title: Comparative and functional analysis of plasma membrane-derived extracellular vesicles from obese vs. nonobese women

Article Type: Full Length Article

Keywords: Exosomal vesicles; microRNAs; plasma; biomarkers; obesity; impaired glucose tolerance

Corresponding Author: Dr. Francisco José Ortega, PhD

Corresponding Author's Institution: IdIBGi

First Author: Fernando SANTAMARIA-MARTOS

Order of Authors: Fernando SANTAMARIA-MARTOS; Iván BENITEZ; Jessica Latorre; Aina LLUCH; José Moreno-Navarrete; Monica Sabater; Wifredo RICART; Manuel SANCHEZ de la TORRE; Silvia Mora; José M Fernández-Real; Francisco José Ortega, PhD

Abstract: Background: Membrane-derived extracellular vesicles (EVs) are released to the circulation by cells found in adipose tissue, transferring microRNAs (miRNAs) that may mediate the adaptive response of recipient cells. This study investigated plasma EVs from obese vs. nonobese women and their functional impact in adipocytes.

Methods: Plasma EVs were isolated by differential centrifugation. Concentration and size were examined by nanoparticle tracking analysis (NanoSight). RNA was purified from plasma and plasma EVs of 45 women (47 ± 12 years, 58% of obesity) and profiles of mature miRNAs were assessed. Functional analyses were performed in human adipocytes.

Findings: Smaller plasma EVs were found in obese when compared to nonobese women. Positive associations were identified between circulating EVs numbers and parameters of impaired glucose tolerance. Almost 40% of plasma cell-free miRNAs were also found in isolated plasma EVs, defined as Ct values<37 in ≥75% of samples. BMI together with parameters of insulin resistance were major contributors to EVs-contained miRNA patterns. Treatments of cultured human adipocytes with EVs from obese women led to a significant reduction of genes involved in lipid biosynthesis, while increasing the expression of IRS1 (12.3%, p=0.002).

Interpretation: Size, concentration and the miRNA cargo of plasma EVs are associated with obesity and parameters of insulin resistance. Plasma EVs may mediate intercellular communication relevant to metabolism in adipocytes.

Opposed Reviewers:

Research Data Related to this Submission

There are no linked research data sets for this submission. The following reason is given:
Data will be made available on request

Clinical Nutrition

Girona (Catalonia, Spain), January 28th, 2019

Dear Editor,

As you certainly may know, since the discovery of membrane-derived extracellular vesicles (EVs) as vehicles for exchange of regulatory microRNAs (miRNAs), RNA-based cell-to-cell communication through plasma EVs has attracted many studies endorsing the idea that EVs and their cargo are of most relevance in physiology and physiopathology. The major challenge is the understanding of how (or whether) RNA-containing circulating EVs induce changes in metabolism and stimulate the response of target cells. So far, the characterization of RNA-based cell-to-cell communication through plasma EVs under physiological conditions is still scarce and needs to be further assessed.

While we previously reported on determinants for obesity and type 2 diabetes of microRNAs found in plasma and adipose tissue [1-8], the study entitled "*Comparative and functional analysis of plasma membrane-derived extracellular vesicles from obese vs. nonobese women*" aimed to investigate their presence in isolated plasma EVs. Thereby, the relation of parameters affecting these biomarkers in obese women and age-matched healthy-weight controls was investigated. Then, functional analyses in human adipocytes were conducted to try to shed additional light on functional differences in lean-obese plasma EVs. This critical step in validation of EVs as functional contributors to metabolic changes accomplished *in vitro* relied on the identification of correlations between clinical outputs and specific EVs-contained miRNA signatures found in obese patients, which, in the future, may be determined in rapid and convenient fashion using EVs-driven biosensors and therapeutical signals leading to cardiometabolic protection against obese-related disturbances.

We believe that this information may be helpful to design strategies to determine and improve the metabolic profile of obese patients, and that this manuscript has high interest for scientific and medical community, and hence for the readers of ***Clinical Nutrition***.

Yours sincerely,

Francisco J. Ortega, Ph.D.
Section of Diabetes, Endocrinology and Nutrition (UDEN)
Girona Biomedical Research Institute (IDIBGI)
Hospital Universitario de Girona Dr. Josep Trueta

1. Latorre J, Moreno-Navarrete JM, Mercader JM, et al. Decreased lipid metabolism but increased FA biosynthesis are coupled with changes in liver microRNAs in obese subjects with NAFLD. *Int J Obes (Lond).* Apr 2017;41(4):620-630.

2. Ortega FJ, Cardona-Alvarado MI, Mercader JM, et al. Circulating profiling reveals the effect of a polyunsaturated fatty acid-enriched diet on common microRNAs. *J Nutr Biochem.* Oct 2015;26(10):1095-1101.

3. Ortega FJ, Mercader JM, Catalan V, et al. Targeting the circulating microRNA signature of obesity. *Clin Chem.* May 2013;59(5):781-792.

4. Ortega FJ, Mercader JM, Moreno-Navarrete JM, et al. Surgery-Induced Weight Loss Is Associated With the Downregulation of Genes Targeted by MicroRNAs in Adipose Tissue. *J Clin Endocrinol Metab.* Nov 2015;100(11):E1467-1476.

5. Ortega FJ, Mercader JM, Moreno-Navarrete JM, et al. Profiling of circulating microRNAs reveals common microRNAs linked to type 2 diabetes that change with insulin sensitization. *Diabetes Care.* 2014;37(5):1375-1383.

6. Ortega FJ, Moreno M, Mercader JM, et al. Inflammation triggers specific microRNA profiles in human adipocytes and macrophages and in their supernatants. *Clin Epigenetics.* 2015;7:49.

7. Ortega FJ, Moreno-Navarrete JM, Pardo G, et al. MiRNA expression profile of human subcutaneous adipose and during adipocyte differentiation. *PLoS One.* Feb 2 2010;5(2):e9022.

8. Prats-Puig A, Ortega FJ, Mercader JM, et al. Changes in circulating microRNAs are associated with childhood obesity. *J Clin Endocrinol Metab.* Oct 2013;98(10):E1655-1660.

Comparative and functional analysis of plasma membrane-derived extracellular vesicles from obese vs. nonobese women

Fernando SANTAMARIA-MARTOS[1], Iván D BENITEZ[1], Jèssica LATORRE[2,3], Aina LLUCH[3], José M MORENO-NAVARRETE[2,3], Mònica SABATER[2,3], Wifredo RICART[2,3], Manuel SANCHEZ de la TORRE[1,4], Silvia MORA[5]*, José M FERNÁNDEZ-REAL[2,3]*, Francisco J ORTEGA[2,3]*

[1] *Group of Translational Research in Respiratory Medicine, Hospital Universitari Arnau de Vilanova y Santa Maria, IRB Lleida – Lleida (Spain)*
[2] *Centro de Investigación Biomédica en Red de la Fisiopatología de la Obesidad y la Nutrición (CIBEROBN), Instituto de Salud Carlos III (ISCIII) – Madrid (Spain)*
[3] *Department of Diabetes, Endocrinology, and Nutrition (UDEN), Institut d'Investigació Biomédica de Girona (IdIBGi) – Girona (Spain)*
[4] *Centro de Investigación Biomédica en Red de Enfermedades Respiratorias (CIBERES), Instituto de Salud Carlos III (ISCIII) – Madrid (Spain)*
[5] *Department of Molecular and Cellular Physiology, Institute of Translational Medicine (ITM), University of Liverpool – Liverpool (UK)*

Running title: Plasma EVs and obesity

Keywords: Exosomal vesicles, microRNAs, plasma, biomarkers, adipocytes, obesity, impaired glucose tolerance, insulin resistance, humans

The authors have nothing to declare. All authors of this manuscript have directly participated in the execution, and analysis of the study. All authors are aware of and agreed to the content of the manuscript and have approved the final version submitted. The contents of this manuscript have not been copyrighted or published previously. There are no directly related manuscripts or abstracts, published or unpublished, by one or more authors of this manuscript. The submitted manuscript nor any similar manuscript, in whole or in part, will be neither copyrighted, submitted, or published elsewhere while the Journal is under consideration.

Abstract word count: **220** words

Word count: **4,868** words

3 Tables and **3** Figures. **5** Supplemental Tables and **5** Supplemental Figures

*Address for correspondence:
F.J. Ortega, Ph.D., J.M. Fernandez-Real, M.D., Ph.D.
Department of Diabetes, Endocrinology, and Nutrition (UDEN)
Institut d'Investigació Biomédica de Girona (IdIBGi)
Hospital of Girona "Dr Josep Trueta", Carretera de França s/n. 17007 - Girona, SPAIN
Phone: +34 628 86 14 78 / e-mail: fortega@idibgi.org, jmfreal@idibgi.org

Silvia Mora, Ph.D.
Department of Molecular and Cellular Physiology
Institute of Translational Medicine (ITM)
University of Liverpool, L69 3BX - Liverpool, UK
Phone: +44 7847 110592 / e-mail: s.mora@liverpool.ac.uk

ABSTRACT

Background: Membrane-derived extracellular vesicles (EVs) are released to the circulation by cells found in adipose tissue, transferring microRNAs (miRNAs) that may mediate the adaptive response of recipient cells. This study investigated plasma EVs from obese vs. nonobese women and their functional impact in adipocytes.

Methods: Plasma EVs were isolated by differential centrifugation. Concentration and size were examined by nanoparticle tracking analysis (NanoSight). RNA was purified from plasma and plasma EVs of 45 women (47 ± 12 years, 58% of obesity) and profiles of mature miRNAs were assessed. Functional analyses were performed in human adipocytes.

Findings: Smaller plasma EVs were found in obese when compared to nonobese women. Positive associations were identified between circulating EVs numbers and parameters of impaired glucose tolerance. Almost 40% of plasma cell-free miRNAs were also found in isolated plasma EVs, defined as Ct values<37 in ≥75% of samples. BMI together with parameters of insulin resistance were major contributors to EVs-contained miRNA patterns. Treatments of cultured human adipocytes with EVs from obese women led to a significant reduction of genes involved in lipid biosynthesis, while increasing the expression of *IRS1* (12.3%, p=0.002).

Interpretation: Size, concentration and the miRNA cargo of plasma EVs are associated with obesity and parameters of insulin resistance. Plasma EVs may mediate intercellular communication relevant to metabolism in adipocytes.

Funding: SAF2015-66312 (FIS, to JMF-R), CIBEROBN (ISCIII), PERIS 2016, 440/C/2016 (MTV3, to FJO), FI-DGR 2015 (AGAUR, to JL), FEDER.

INTRODUCTION

Cells can release to the circulation membrane-embedded extracellular vesicles (EVs) that, based on their composition, nature and size, are grouped into different classes. The majority of EVs occur within the sub-micron range (30–1,000 nm), where small vesicles of different origin appear to be the most abundant EVs subclass, present in the lowest size range (≤200 nm) **[1]**. EVs from human plasma are a mixture of microparticles, exosomes, and other vesicular structures. The potential of plasma EVs for diagnosis and prognosis of different diseases is being intensely investigated, as changes in circulating EVs may give important information related to silent disease and early metabolic impairment **[2]**. Notably, elevated concentration of plasma EVs have been identified in a number of pathological disorders, including cardiovascular disease **[3]**. The association between adiposity, EVs-markers, and metabolic syndrome has been tested in patients with clinically manifest vascular disease, in association with subcutaneous and visceral fatness **[4]**. On the other hand, *in vitro* and *in vivo* treatments with plasma microparticles from patients with metabolic syndrome provided evidence that circulating EVs may influence endothelial dysfunction to some extent **[5]**.

To the best of our knowledge, none of the previous studies have investigated the relationship between circulating EVs' properties and clinical parameters in subjects without manifest cardiovascular or metabolic disease. The aim of this work was to characterize circulating EVs obtained from a group of healthy lean and obese women and determine the biophysical properties and the miRNA content of these EVs. Then, we provide some functional analysis in human adipocytes to ascertain their activity in regulating gene expression in recipient cells as previously **[6]**, as a proxy of their functionality. We also provide a comparison of the miRNA EVs content to that of the whole plasma miRNA profiles in these individuals. Our results suggest that circulating EVs have distinct biophysical and contain biological molecules capable of regulating gene expression relevant to metabolism in human adipocytes.

RESEARCH DESIGN AND METHODS

Subject recruitment

Forty-five women aged between 30 and 70 year-old (47 ± 12 years), including 58% of obesity (body mass index (BMI) ≥ 30 kg/m^2), were enrolled at the Endocrinology Service of the Hospital Universitari Dr. Josep Trueta de Girona (Girona, Spain) for plasma membrane-derived extracellular vesicles (EVs) isolation and microRNA (miRNA) profiling in both plasma and isolated plasma EVs. Inclusion criteria were i) absence of acute or systemic disease, and ii) absence of infection within the previous month. None of the subjects recruited were under medication or had evidence of metabolic disease. Liver disease and thyroid dysfunction were specifically excluded by biochemical work-up.

Clinical measurements

BMI was calculated as weight (in kilograms) divided by height (in meters) squared. Percent fat mass was measured using the Tanita BIA scale (Tanita Corporation, Tokyo, Japan). The subjects' waist was measured with a soft tape midway between the lowest rib and the iliac crest. The hip circumference was measured at the widest part of the gluteal region. The waist-to-hip (WtH) ratio was then calculated. Blood pressure was measured in the supine position on the right arm after a 10-min rest. A standard sphygmomanometer of appropriate cuff size was used and the first and fifth phases were recorded. Values used in the analysis are the average of three readings taken at 5 min intervals. Blood samples were withdrawn after an overnight fast between 8:00 and 9:00 a.m. Serum glucose was measured in duplicate by the glucose oxidase method with a Beckman Glucose Analyzer 2 (Brea, CA). The coefficient of variation (CV) was 1.9%. Serum insulin was measured in duplicate using a monoclonal immunoradiometric assay (Medgenix Diagnostics, Fleunes, Belgium). The inter and intra-assay CVs were 6.9 and 4.5% at 14 and 89 µIU/l, respectively. Insulin resistance was calculated in all subjects using the HOMA-IR value [glucose (mmol/l) × insulin (µIU/l) / 22.5], as previously described **[7]**. Lipid profile

(triglycerides, total cholesterol, and high and low-density lipoproteins) were measured by enzymatic methods on a Hitachi 917 instrument (Roche, Mannheim, Germany). Whole blood hemoglobin levels (EDTA sample, Coulter Electronics, Hialeah, FL) were determined by routine laboratory tests. Glycated hemoglobin (HbA1c) was measured by the high-performance liquid chromatography method (Bio-Rad, Muenchen, Germany). Intra and inter-assay CVs were less than 4% for all these tests. High-sensitive C reactive protein (CRP) was measured by a turbidimetric assay on the Integra 800 analyser (Roche). Participants were requested to withhold alcohol and caffeine for at least 12 h prior to the different tests, and were non-smokers.

Isolation and characterization of plasma EVs

Plasma was obtained by standard venepuncture and centrifugation using EDTA-coated Vacutainer tubes (Becton-Dickinson, Franklin Lakes, NJ). The separation was performed by double-centrifugation using a laboratory centrifuge (Beckman J-6M Induction Drive Centrifuge, Beckman Instruments Inc., Palo Alto, CA). The first spin was performed at 1,000 × g for 15 min at 4ºC. The second spin was performed at 2,000 × g for 5 min at 4ºC. Plasma samples from each participant were processed to isolate circulating EVs, as previously described **[8]**. Briefly, 5 ml of plasma EDTA were diluted with 15 ml of cold sterile phosphate buffered saline (PBS) and centrifuged twice, at 2,000 × g and 12,000 × g for 45 min, to remove any remaining cellular debris. Then, supernatants were collected and ultracentrifuged at 100,000 × g 4ºC for 140 min. Next, supernatants were discarded and pellets were resuspended in 10 ml of cold PBS, before a filtering step using sterile 10 ml syringes and 0.22 μm adjustable filters. Additional ultracentrifugation of 75 min was carried out at 100,000 × g and 4°C. Finally, pellets of plasma EVs were resuspended with 100 μl of cold and sterile PBS, aliquoted and stored at -80ºC until subsequent analysis and characterization, RNA extraction and functional tests.

For transmission electron microscopy (TEM), isolated small plasma EVs suspensions were fixed in 4% paraformaldehyde for 60 min. EVs suspensions from 6 different samples (approximately 10 μl) were applied to copper mesh Formvar coated carbon stabilized grids, were allowed to adsorb to the grid for 20 min and then were wicked off with filter paper. For

negative staining, 1% Aqueous Uranyl Acetate (10 µl) was applied to the grid for 2 min, then wicked off with Whatman filter paper. Grids were allowed to thoroughly dry before viewing (**Figure 1A**) with a JEOL JEM 1010 transmission electron microscope (JEOL USA Inc., Peabody, MA), operated at 80 kV and equipped with a SC1000 ORIUS® CCD Camera (Gatan Inc., Pleasanton, CA). Nanoparticle tracking analysis (NTA) is a powerful technique that combines the properties of laser light scattering microscopy and Brownian motion, in order to obtain size and distribution of microparticles in liquid suspension **[9]**. Plasma EVs size distribution and concentrations were determined by means of a Malvern Nanosight NS300 Instrument (Malvern Instruments Ltd, UK), as explained by Vestad *et al*. **[10]**. Dilutions of 1:200 in PBS were injected into the NanoSight chamber. The camera gain was set at a constant value of 10, and the threshold value for microvesicle detection was set at 5. The NTA intra-assay (i.e. within-day, n=16) variation was as follows (mean ± SE, min.-max.): particle concentration (particles/ml): 713,625,000 ± 41,024,583 (259,000,000-1,310,000,000); particles per frame: 36 ± 2 (13-67); centers per frame: 39 ± 3 (15-66); particle mean diameter: 118.92 ± 4.6 (101.5-137). Inter-assay (day-to-day, n=5) coefficients of variation for plasma EVs preparations ranged from 5% to 20%. Results were retrospectively studied in association with anthropometrical and biochemical variables, and were used for normalizing the amount of EVs suspension and plasma sample used in each experiment.

MicroRNA profiling in plasma and isolated plasma EVs

Total RNA content was extracted from ~2 million plasma EVs and an equivalent amount of paired-plasma samples by methods aimed at preserving and isolate small RNA molecules (mirVana PARIS Isolation Kit, Applied Biosystems, Darmstadt, Germany). A fixed volume of 3 µl RNA solution from the 40 µl-eluate was used as input into the reverse transcription (RT), using the TaqMan miRNA Reverse Transcription Kit and the TaqMan miRNA Multiplex RT Assays, which are required to run the TaqMan® Array human MicroRNA A+B Cards Set v2.0 (Life Technology, Darmstadt, Germany). Pre-amplification was performed using TaqMan PreAmp Master Mix and Megaplex™ PreAmp Primers for either human Pool Set A and B,

which provide an optional pre-amplification step prior to real-time analysis when sensitivity is of the utmost importance and/or the sample is limiting. Profiling of 754 mature miRNA species was carried out by means of Taqman low density array cards, as previously explained **[11, 12]**. The screening was performed in 6 pools of samples, comprised of either isolated EVs or paired-plasma samples, so 12 miRNA arrays were carried out. Plasma and isolated plasma EVs from each participant were merged together before sample processing and miRNA profiling. The identification subgroup was comprised of 18 carefully preselected participants. The characteristics of the subjects that were eligible for pooling and miRNA profiling are shown in **Supplemental Table 1**. Samples were pooled together in groups of three. These pools were intended to be representative for each study group (3 obese vs. 3 nonobese groups). Three pools were aimed at identifying miRNAs contained in obese EVs (BMI ≥ 30 kg/m2), while the other three were comprised of samples from lean participants (BMI < 25 kg/m2). Semi quantitative real time-PCR was carried out on an Applied BioSystems 7900HT thermocycler. Data was analyzed with SDS Relative Quantification Software version 2.2.2, with an assigned minimum threshold above the baseline of all assays showing measurable amplification above background. In this discovery samples, "mean" normalized values ("DeltaCt") were obtained as the raw Ct value – average of raw Cts for all miRNAs with reliable results (Ct values ≤ 37) in each pool (**Supplemental Figure 1**). The "relative quantification" measures the presence of specific miRNAs and is calculated in each sample as $2^{(-\text{"DeltaCt"})}$ for each sample. Fold-changes reflect differences for values of this "relative expression" between groups of subjects.

Commercially available TaqMan hydrolysis probes (Applied Biosystems, Darmstadt, Germany; **Supplemental Table 2**) were used to assess the presence of individual miRNA candidates in all samples (n=45). The pre-amplification product was diluted 1:200 previous being combined (5 μL) with 0.25 μL of TaqMan miRNA hydrolysis probes (20x), and 4.75 μL of the LightCycler 480 Probes master mix (2x) (Roche Diagnostics, Barcelona, Spain) to a final volume of 10 μL. Gene expression was assessed by real-time PCR using the LightCycler® 480 Real-Time PCR System (Roche Diagnostics, Barcelona, Spain). For the analysis by qRT-PCR, we evaluated first a suitable number of reference (or "housekeeping") miRNAs, based on their

expression stability, and according to the GeNorm methodology implemented in the R package SL qpcrNorm (Bioconductor) **[13]**. Then, we used "DeltaCt" normalization procedures based on the most stable (or "rank invariant") miRNAs in plasma EVs, as implemented in the HTqPCR R package **[14]**. Thus, the geometric mean of these selected internal controls (i.e. miR-30c, miR-24, and miR-484) was used as reference, as previously reported **[15]**. All analyses were carried out in parallel within the same day. We excluded Ct values higher than 37 in the semi-quantitative assessment, and higher than 34 when evaluating the qualitative enrichment of EVs-contained miRNAs. Three qRT-PCR replicates and positive and negative controls were included in all reactions. Intra-assay coefficients of variation were less than 12% for the most prevalent miRNAs in plasma EVs (i.e. miR-320, miR-186-3p, miR-323-3p, miR-106a, let-7b, miR-186, miR-146a, miR-106b).

Impact of plasma EVs on human adipocytes: changes in gene expression

Two thousand human subcutaneous preadipocytes from a non-diabetic Caucasian male with BMI < 30 kg/m^2 and age < 40 y (Zen-Bio Inc., Research Triangle Park, NC) were cultured with Preadipocytes Medium (PM, Zen-Bio Inc.) in a humidified 37ºC incubator with 5% CO_2. Twenty-four hours after plating cells in 12-well culture plates, preadipocytes were checked for confluence and differentiated using the commercially available Differentiation Medium (DM, Zen-Bio Inc.), following manufacturer's instructions. Non-differentiated preadipocytes used as control for adipogenesis were maintained in PM. Two weeks after initializing differentiation, differentiated cells appeared rounded with large lipid droplets apparent in the cytoplasm. Cells were then considered mature adipocytes and incubated with fresh adipocytes medium containing ~250,000 plasma EVs/µl. These EVs were obtained from 6 obese and 6 lean women to assess functional differences regarding the impact *in vitro* of plasma obese-lean EVs. In parallel, THP-1 macrophages were treated for 24 h with 10 ng/ml lipopolysaccharide (LPS) obtained from *Escherichia coli* O111:B4 (Sigma Chemical Co.). The LPS-stimulated macrophage conditioned media (MCM) was collected and centrifuged at 400 × g for 5 min, diluted with adipocyte medium (2%) and used to induce in differentiated human adipocytes the

chronic low-grade inflammation state of obesity, as we have previously reported **[12]**. After 24 h of treatment, cells were removed and stored at -80ºC for future analysis.

Total RNA was purified from cells using miRNeasy® Mini Kit (QIAgen, Gaithersburg, MD). Cells were homogenized in 0.6 mL of QIAzol® Lysis Reagent (QIAgen), a monophasic solution of phenol and guanidine thiocyanate which facilitates sample disaggregation and inhibits RNAses. After addition of chloroform (0.4 volumes), the homogenate was separated into aqueous and organic phases by centrifugation (15 min at 12,000 × g and 4ºC). Then, the upper aqueous phase was isolated and ethanol absolute (1.5 volumes) was added, to provide appropriate binding conditions for RNA molecules. The sample was applied to a silica-membrane RNeasy spin columns, where RNA binds to the membrane while phenols and other compounds are washed away. High quality RNA was finally eluted in 30 μL of RNAse-free water. Final RNA concentrations were assessed with a Nanodrop ND-1000 Spectrophotometer (Thermo Fischer Scientific, Wilmington, DE). The integrity was checked with the Nano lab-on-a-chip assay for total eukaryotic RNA using Bioanalyzer 2100 (Agilent Technologies, Palo Alto, CA). The RNA integrity number (RIN) obtained was above 8 for all replicates.

Three μg of total RNA were reverse transcribed to cDNA using High Capacity cDNA® Archive Kit (Applied Biosystems, Darmstadt, Germany) according to the manufacturers' protocol. Expression was assessed by real time PCR using the LightCycler® 480 Real-Time PCR System (Roche Diagnostics, Barcelona, Spain), and TaqMan® technology suitable for relative gene expression quantification. The reaction was performed following manufacturers' instructions in a final volume of 7 μL. The cycle program consisted of an initial denaturing of 10 min at 95ºC then 45 cycles of 15 sec denaturizing phase at 92ºC and 1 min annealing and extension phase at 60ºC. Then, the crossing points (Cp) values were assessed for each amplification curve by the Second Derivative Maximum Method. The "DeltaCp" value was calculated by subtracting the Cp value for the corresponding endogenous controls in each sample from the Cp value for each target gene. Fold changes compared with the endogenous control were then determined by calculating $2^{(-\text{"DeltaCp"})}$, so gene expression results are expressed as expression ratio relative to preselected and validated housekeeping. The peptidyl-prolyl cis-

trans isomerase A (PPIA), also known as cyclophilin A, was assessed as the most suitable endogenous control for gene expression in adipocytes **[16]**. The commercially available TaqMan® primer/probe sets used for measures of gene expression are listed in the **Supplemental Table 2**. Replicates and positive and negative controls were included in each reaction.

Statistical analyses

Descriptive results of continuous variables are expressed as mean ± standard deviation (SD). Before statistical analysis, normal distribution and homogeneity of the variances were evaluated using Levene's test. ANOVA and paired *t*-tests were performed to study differences on quantitative variables between groups. The semi-quantitative concentrations for the different miRNAs were correlated with clinical parameters (Spearman's test). Multiple linear regression models in a stepwise manner were constructed to evaluate the independent contribution of specific variables. Data analyses were performed with the SPSS statistical software (SPSS V12.0 Inc., Chicago, IL), and the *R* Statistical Software (http://www.r-project.org/). miRNA targeting sequences within the miRNA sequence were checked using miRBase (http://www.mirbase.org/). Predicted target transcripts of miRNA candidates were collected and combined from databases such as TargetScanHuman (http://www.targetscan.org/), miRNA.org, and miRWalk (www.ma.uniheidelberg.de). In addition, blastn (http://www.clustal.org/) was used to detect additional similarities which were 7 base pairs or longer, and we explored the web-based repository TissueAtlas (https://ccb-web.cs.uni-saarland.de/tissueatlas) in order to assess the tissue origin of miRNAs contained in EVs.

RESULTS

Plasma EVs size and concentration are associated with obesity and parameters of impaired glucose tolerance

The clinical characteristics of the 45 healthy women are shown in **Table 1**. Significant variations in particle size distribution (**Figure 1B**) depicted fairly smaller plasma extracellular vesicles (EVs) in women with grade I obesity (body mass index (BMI) of 30-35 kg/m^2) (116.7 ± 9.1 nm), and in women with BMI ≥ 35 kg/m^2 (114.3 ± 8.6 nm), when compared to lean (122.6 ± 5 nm) and overweight (124.6 ± 8.2 nm) participants (**Figure 1C**). Significant inverse associations (Spearman's) were found between EVs diameter, BMI (r=-0.53, p=0.0002; **Figure 1D**), and waist circumference (r=-0.43, p=0.014). The size of plasma EVs also correlated with fasting triglycerides, fasting insulin, and HOMA-IR, while being positively associated with HDL cholesterol (**Table 2**). BMI (p=0.014) and fasting triglycerides (p=0.045) contributed to explain 33.8% (p=0.001) of plasma EVs size, after controlling for age and fasting insulin in multiple linear regression models. On the other hand, independent and positive associations were identified between circulating concentrations of EVs and parameters of impaired glucose tolerance, such as fasting glucose (r=0.51, p=0.0006; **Figure 1E**) and glycated hemoglobin (r=0.32, p=0.042; **Table 1**). Interestingly, fasting glucose alone (p=0.002) accounted for 21.1% (p=0.007) of the variance in plasma EVs concentration, after adjusting for age and BMI. Altogether, current results point at significant differences affecting plasma EVs and being intrinsically and independently linked to increased fatness (size) and parameters of impaired glucose tolerance (concentration) in apparently healthy women.

Plasma EVs-contained miRNA patterns are associated with obesity and HOMA-IR

Plasma EVs-contained miRNA profiling was performed in plasma samples of 18 subjects that were merged together in 6 groups (3 obese vs. 3 nonobese groups) as detailed in the methods section. The characteristics of these participants are detailed in **Supplemental Table 1**. In this

identification sample, one hundred miRNAs (± 16) showed Ct values <37 in isolated EVs. Under same conditions of RNA extraction, analysis and clustering, whole plasma showed 264 (± 44) mature miRNA species, including the miRNAs found in isolated plasma EVs. No significant differences were identified between groups of subjects for the absolute amounts of RNA, or the number of miRNAs that can be quantified under such conditions (**Supplemental Figure 2A**). However, heatmap and clustering of miRNAs detection in EVs (but not in plasma) pointed out the existence of three groups of samples, instead of two (**Supplemental Figure 2B**). Conversely, BMI and parameters of insulin resistance such as fasting insulin and HOMA-IR seemed to be major contributors to miRNA patterns in plasma EVs (**Figure 2**).

One important question was whether miRNA profiles assessed in EVs may indicate some sort of "selectivity" for miRNAs enriched within circulating EVs, with regard to the overall plasma miRNA population, as previously postulated **[17]**. To address this key question, we strengthened the conditions under which we considered indisputable the presence of miRNAs in both plasma and isolated plasma EVs, or only in plasma, now defined as Ct values < 35 in all samples. Thereby, the recovery of 18% of plasma cell-free miRNAs was also prevalent in isolated plasma EVs of at least one group (**Supplemental Figure 3**). With these curated lists of miRNAs, we investigated whether there was a specific sequence in the subset of miRNAs that would be enriched in plasma EVs, which may act like a "zipcode" to target them into EVs **[17]**. However, the multiple sequence alignment analysis comparing the miRNAs found in plasma EVs revealed not common sequences explaining such enrichment (**Supplemental Figure 3**). On the other hand, we used these lists to dig into the tissue origin of plasma EVs-contained miRNAs. As previously described in **[18]**, the majority of these miRNAs fell in amiddle tissue specificity index (TSI) ranges, and was not specific for single tissues. Nonetheless, among EVs-contained miRNAs we observed miRNAs and miRNA families that were predominantly expressed in certain tissues, such as veins, thyroid gland, lung, skin, and also in adipocytes (e.g. MIR-17 family, **Supplemental Figure 4**), indicating these tissues as potential contributors to the miRNA repertoire of human plasma EVs. Obviously, such conclusions need to be further endorsed in additional follow-up studies.

Finally, miRNA candidates were analyzed in each sample, including the subjects selected for pooling and miRNA profiling. These validation procedures with individual assays shortlisted a subset of 8 EVs miRNAs that significantly differed between groups (**Table 1**). In partial agreement, EVs-associated miRNA candidates were associated with BMI, while others showed significant and independent association with biomarkers of incipient impaired glucose tolerance (e.g. fasting glucose, glycated hemoglobin), insulin resistance (fasting insulin, HOMA-IR), inflammation (C reactive protein), and dyslipidemia (fasting triglycerides, cholesterol) (**Table 3**).

Impact of plasma EVs on gene expression in adipocytes

Obesity leads to adipose tissue dysfunction, with deranged expression of adipokines and genes involved in glucose and lipid metabolism, resulting in insulin resistance and inflammation. We previously found that EVs from obese subjects impair insulin stimulated glucose uptake in cultured adipose cells **[6]**. To gather further insights into the biological effects of these EV isolated from obese and lean women, we sought to determine the changes in gene expression in adipose cells that may occur by direct transfer of miRNAs and other molecules found in these EVs. Therefore, we tested the hypothesis that EVs present in plasma of obese individuals may alter the expression of cytokines, reducing the production of insulin sensitizing factors and increasing the synthesis of molecules that may modulate metabolism in lipid-containing differentiated adipocytes. Acute treatments of 24 h with plasma EVs of obese women lead to significant reduction in the expression of genes involved in adipogenesis (e.g. *GLUT4*, *ADIPOR1*, *CEBPA*) and fatty acid biosynthesis (*ACLY*, *ACACA*, *FASN*, *ELOVL6*), while increasing the expression of *IRS1* (12.3%, p=0.002), when compared to EVs of lean participants (**Figure 3**). Additional associations pointed the interrelationship between the BMI of donors and changes in the expression of *CEBPA*, *FASN*, *GLUT4*, *IRS1*, and *ACLY*, while measures of increased insulin resistance accounted for increased *GLUT4*, *IRS1*, and *FASN*, and decreased *IL6*, *SREBF1*, and *ELOVL6* gene expression in adipocytes (**Supplemental Table 4**).

DISCUSSION

Since the discovery of plasma membrane-derived extracellular vesicles (EVs) as "vehicles" for exchange of regulatory microRNAs (miRNAs), RNA-based cell-to-cell communication through EVs has attracted many studies endorsing the concept that circulating EVs and their cargo are of most relevance in physiology and physiopathology **[19, 20]**. Many of these EVs are released to the circulation by a variety of cells found in adipose tissue **[21]**, including macrophages **[22]**, mesenchymal stem cells **[23, 24]**, and adipocytes **[21, 25, 26]**. These plasma EVs may elicit both autocrine and paracrine effects but information regarding their distribution size, concentration and miRNA content in obese subjects is scarcely available and could provide important information to understand the development of metabolic syndrome in this population.

Trying to determine the extent to which obesity contributes to plasma EVs and EVs-contained miRNAs, we isolated EVs from the plasma of 45 women who varied widely in terms of obesity and fat mass (14 to 66% of their body weight). Then, we dissected differences regarding plasma EVs size, concentration and the miRNA content among lean, overweight, and obese participants. These circulating vesicles were fairly smaller in obese women than in nonobese participants. Interestingly, the number of small EVs isolated from obese and lean participants was equivalent, but differed according to biomarkers of impaired glucose tolerance, such as fasting glucose and glycated hemoglobin. In agreement with this piece of data, genetically obese *ob/ob* mice displayed elevated numbers of circulating EVs when compared to lean wild-type controls **[27]**, and an increased secretion of EVs was achievable in adipocytes following exposure to biological stimuli related to the chronic low-grade inflammation state of obesity, even though no variations in size were reported **[28]**. On the other hand, higher circulating levels of EVs have been found in obese patients **[29]**, suggesting that enlarged fat depots may contribute to such increase. In agreement, EVs size distribution and concentrations indicated a nominal increase in the frequency of small EVs found in diabetic rats and humans **[30]**. Plasma EVs concentrations were also two-fold greater in gestational diabetic women,

when compared to matched pregnancies with normal glucose tolerance **[31]**. The current study identified significant variations in circulating EVs concentrations and size in close association with the BMI and parameters of glucose tolerance of apparently healthy women. From a clinical point of view, the results obtained here give promising evidence for future analyses using plasma EVs as an early and non-invasive diagnosis of obesity-associated metabolic disturbances. Obviously, additional studies are needed to confirm these associations.

Relevance of miRNAs-containing plasma EVs in obesity

Some of the abilities for fine-tuned regulation of metabolic properties have been ascribed to the miRNAs contained in adipose-derived plasma EVs **[21]**. Thus, monitoring expression signatures affected by plasma EVs from obese/lean subjects in cellular systems may shed some light on pathways that are regulated by circulating EVs targeting recipient cells. In this respect, different profiles of EVs containing miRNAs have been identified in mice feeding high-fat diet and leptin-deficient obese models, when compared to lean wild-type animals **[25]**. The study of Thomou *et al.* **[21]** pointed at the adipose tissue as a major source of circulating EVs-contained miRNAs, and demonstrated that adipocyte-derived circulating miRNAs are contained in plasma EVs that may display physiological functions in neighboring cells and farther tissues. These findings uncovered the potential role of adipose-derived miRNA-containing plasma EVs in the pathogenesis of metabolic diseases.

PCR analyses with reverse transcription profiling of plasma EVs revealed the presence in plasma EVs of at least one-hundred miRNAs, accounting for around one third of the miRNAs that can be quantified in whole plasma. Here again, different profiles of miRNAs in plasma EVs were independently associated with BMI and parameters of insulin resistance. Previously, plasma exosome miRNA profiling unraveled 3 potential modulators of adiponectin in diabetes, affecting the glycemic index in poorly controlled diabetic patients **[32]**. In inflammatory microvesicles, miR-133, let-7, miR-17/92, miR-21, miR-29, miR-126, miR-146, and miR-155 were found in association with metabolic and cardiovascular diseases **[33]**. An independent study revealed significant reduction of miR-126 in circulating EVs of patients with stable

coronary artery disease **[34]**. A group of miRNAs, including miR-21 and miR-126, was also up-regulated in plasma EVs isolated from subjects with vulnerable coronary artery disease **[35]**. Our results, assessed in a well-characterized sample of apparently healthy women, identified at least 8 EVs-contained miRNA candidates related to BMI (e.g. let-7b, miR-146a), and showed discordant profiles linked to dislipidemia (miR-29c) and values of insulin resistance, including three miRNAs significantly associated with fasting insulin (i.e. miR-222/223, miR-26b). Thereby, the levels of circulating EVs-contained miRNAs might represent a fine-tuned biomarker of slightly variations in insulin sensitivity that may account in parallel to (or independently of) increased fat depots.

Obese plasma EVs may compromise adipocyte commitment *in vitro*

Even thought body tissues are exposed to plasma EVs of different origins, making difficult the analysis of specific contributions for each subset of EVs, plasma samples from obese patients are enriched in adipose-derived EVs, as previously indicated **[27-29]**. Conversely, adipocyte-released EVs have shown autocrine functions **[6, 36]**, regulating lipid deposition, proliferation, inflammation, the metabolism of neighboring cells, and modulation of the adaptive response in tissues and organs reached through the circulation **[37]**.

By treating cell cultures of adipocytes from the same donor with isolated plasma EVs from lean and obese women it was possible to characterize the contribution of circulating EVs to the inflammatory and metabolic state of adipocytes exposed to this plasma content. These experimental procedures were aimed at unravel the relevance of obese EVs in energy homeostasis and impaired metabolism. This critical step in validation of EVs as functional contributors to metabolic changes accomplished *in vitro* relied on the identification of correlations between clinical outputs and specific EVs-contained miRNAs found in obese patients. Thereby, 24 h of treatment with obese plasma EVs significantly reduced the expression of genes related to lipogenesis, without modifying neither inflammatory nor lipolytic aspects, when compared to lean EVs. Interestingly, only *IRS1* showed increased expression in human adipocytes treated with plasma EVs from obese women, being more likely related to the fasting

insulin levels of these participants, which also correlated with changes in *GLUT4* and *FASN*. In fact, plasma EVs showed different functional properties according not only to the fatness of the donors but also to biochemical aspects mirroring decreased insulin sensitivity. Moreover, the interpretation of miRNAs significantly up-regulated in obese EVs (e.g. hsa-miR-155-5p, hsa-let-7b-5p, hsa-miR-146a/b-5p, hsa-miR-892b) identified target genes involved in fatty acid alpha oxidation and in both IGF1 and leptin signaling, through the potential modulation of experimentally validated target genes such as *PTGS2* and *STAT3*. On the other hand, miR-301a-3p and miR-145-5p were more likely found in plasma EVs from lean participants, and disclosed their specific involvement in leptin and the insulin receptor signaling through the ability of modulate *PDE3B* gene expression (**Supplemental Table 5**). To test this hypothesis, we evaluated whether genes harboring miRNA target sites for these miRNA candidates were differentially modulated in treated adipocytes. However, gene expression of these targets changed little if any in adipocytes under treatment with lean/obese EVs. In fact, changes affecting these genes in cell cultures were more likely related to metabolical outputs (**Supplemental Table 4**) than to the weight of donors or the presence/abundance of miRNA candidates. This points out the intricate nature of these "vehicles", with dozens of regulatory miRNAs showing variations at both the qualitative (presence/absence) and quantitative (relative abundance) level, and suggests alternative mechanisms leading to the acute regulation of gene expression in adipocyte cultures under treatment with plasma EVs. Additional studies are needed before any more definite conclusion can be drawn.

Conclusions

Plasma EVs may contribute to energy homeostasis, being involved in metabolic disease development and progression, and may provide useful biomarkers for impaired metabolism. By deciphering the processes of physiological communication through EVs found in circulation, the understanding of mechanisms conducting to obesity-related morbidities may be unveiled. We report that in women with no clinically manifest of cardiovascular or metabolic disease, plasma EVs concentration, size and miRNA cargo were independently related to obesity and

parameters of insulin sensitivity. Concurrently, obese plasma EVs blunted the expression of genes involved in the synthesis of lipids in human adipocytes, compromising their activity *in vitro*. Altogether, current results identify miRNAs present in EVs during obesity in the absence of onset of disease, and suggest potential mechanisms underlying the role of plasma EVs in the development of adipose tissue dysfunction in obesity, paving the way for the development of new therapies and applications.

Author Contribution: FS-M, AL, JMM-N, JL, and MS analyzed biochemical variables. FS-M and IB participated in the statistical analysis. WR and MST provided support, reagents, and intellectual content. SM, JMF-R, and FJO designed the study, participated in the analysis of biochemical variables, performed statistical analysis, and wrote the manuscript.

Acknowledgments: Electron microscopy characterization has been carried out using TEM facilities of the "Scientific and Technological Centers" (*Universitat de Barcelona*, CCiT-UB), School of Medicine, *Hospital Clínic de Barcelona*. This study was supported by research funds from the *Ministerio de Educación y Ciencia* (SAF2015-66312, to JMF-R), the *Instituto de Salud Carlos III* (CIBEROBN), and by grants from the *Govern de la Generalitat* (*Pla Estratègic de Recerca i Innovació en Salut*, PERIS 2016) and from the *Fundació La Marató de TV3* (440/C/2016, to FJO), the *Agència de Gestió d'Ajuts Universitaris de Recerca* (AGAUR, FI-DGR 2015, to JL), and the *Fondo Europeo de Desarrollo Regional* (FEDER). Francisco J Ortega was also supported by an award from the Daniel Bravo Andreu Private Foundation.

Table 1 Anthropometrical and biochemical characteristics of study women.

All subjects	**BMI<30 kg/m^2**	**30≤BMI<35 kg/m^2**	**BMI≥35 kg/m^2**	**ANOVA**	**p-value[a]**
N (women)	19	12	14		
Age (years)	45.1 ± 15.1	49.9 ± 11.3	46 ± 8.8	0.574	0.848
BMI (kg/m^2)	24.8 ± 2.7	32.2 ± 1.5	38 ± 3.9	**<0.0001**	**<0.0001**
Fat mass (%)	24.3 ± 4.2	42.1 ± 14.6	50.1 ± 13.1	**<0.0001**	**<0.0001**
Waist (cm)	82.6 ± 9.0	94.7 ± 4.3	99.4 ± 5	**<0.0001**	**<0.0001**
Hip (cm)	96.4 ± 6.1	106.5 ± 5.1	112.8 ± 2.9	**<0.0001**	**<0.0001**
WtH ratio	0.87 ± 0.08	0.89 ± 0.03	0.88 ± 0.05	0.633	0.591
SBP (mm Hg)	133.7 ± 25.7	125.3 ± 17.1	127.9 ± 8.9	0.510	0.442
DBP (mm Hg)	77.2 ± 10.3	79.6 ± 7.3	78.1 ± 5.2	0.745	0.769
Fasting glucose (mg/dl)	88.0 ± 9.3	92.2 ± 8.8	88.1 ± 13.4	0.562	0.984
Insulin (µIU/ml)	5.25 ± 2.34	7.79 ± 3.02	7.86 ± 3.58	**0.022**	**0.016**
HOMA-IR	0.97 ± 0.47	1.64 ± 0.75	1.74 ± 0.73	**0.035**	**0.017**
Glycated haemoglobin (%)	4.59 ± 0.39	4.91 ± 0.3	4.95 ± 0.59	0.075	**0.036**
Cholesterol (mg/dl)	200.7 ± 30.4	214.3 ± 50.9	208.9 ± 30	0.626	0.549
HDL Cholesterol (mg/dl)	72.2 ± 14.3	60.8 ± 13.6	55 ± 9.9	**0.002**	**0.001**
LDL Cholesterol (mg/dl)	112.3 ± 32.1	134 ± 43.4	134.9 ± 29.4	0.147	0.084
Triglycerides (mg/dl)	80.6 ± 32.1	97.5 ± 54.8	95 ± 37.8	0.497	0.347
Mean EVs diameter (nm)	123.5 ± 6.6	116.7 ± 9.1	114.3 ± 8.6	**0.005**	**0.002**
EVs/ml plasma (x 10^6)	4,394 ± 1391	3,964 ± 1824	4,378 ± 1549	0.725	0.977
miR-320a-3p in EVs	0.1427 ± 0.1094	0.1485 ± 0.1064	0.3526 ± 0.2299	**0.002**	**<0.001**
let-7b-5p in EVs	0.0271 ± 0.0278	0.0314 ± 0.0268	0.0934 ± 0.0863	**0.004**	**0.001**
miR-186-3p in EVs	0.1 ± 0.071	0.0456 ± 0.0628	0.033 ± 0.0339	**0.01**	**0.004**
miR-106a-5p in EVs	37.4 ± 29.46	75.51 ± 50.99	68.11 ± 38.51	**0.02**	**0.022**
miR-323a-3p in EVs	0.6621 ± 0.6229	1.6962 ± 1.1418	1.1332 ± 0.96	**0.024**	0.117
miR-146a-5p in EVs	0.2084 ± 0.1051	0.1709 ± 0.1171	0.1193 ± 0.0608	0.056	**0.017**
miR-186-3p in EVs	0.0114 ± 0.0087	0.0049 ± 0.0039	0.0063 ± 0.0044	0.059	**0.046**
miR-106b-5p in EVs	13.97 ± 14.62	21.64 ± 10.5	27.70 ± 25.4	0.116	**0.042**
miR-320a-3p in Plasma	0.0907 ± 0.0902	0.1257 ± 0.0752	0.2363 ± 0.223	0.033	**0.01**
let-7b-5p in Plasma	0.0469 ± 0.0275	0.0404 ± 0.0197	0.0488 ± 0.0229	0.797	0.844
miR-186-3p in Plasma	0.1091 ± 0.0608	0.1047 ± 0.0803	0.0739 ± 0.0163	0.209	0.084
miR-106a-5p in Plasma	1.12 ± 0.39	1.2 ± 0.64	0.97 ± 0.19	0.436	0.304
miR-323a-3p in Plasma	0.0041 ± 0.0029	0.0062 ± 0.0034	0.0086 ± 0.0057	**0.016**	**0.005**
miR-146a-5p in Plasma	1.84 ± 0.8	1.41 ± 1.25	2.56 ± 2.38	0.256	0.19
miR-186-3p in Plasma	0.0412 ± 0.0335	0.0231 ± 0.0123	0.0286 ± 0.0211	0.266	0.222
miR-106b-5p in Plasma	0.0813 ± 0.1012	0.0218 ± 0.016	0.0784 ± 0.1284	0.451	0.938

Results are mean ± standard deviation. **BMI**: Body mass index, **WtH**: Waist to hip, **SBP**: Systolic blood pressure, **DBP**: Diastolic blood pressure, **HOMA-IR:** Homeostatic model assessment of insulin resistance, **HDL**: High-density lipoprotein, **LDL**: Low-density lipoprotein, **EVs**: Extracellular vesicles. **[a]** Fisher's least significant difference (LSD) post-hoc test was performed by comparing subjects with BMI≥35 kg/m^2 vs. non-obese participants (BMI<30 kg/m^2) women. Significant differences ($p<0.05$) are shown in **bold**.

Table 2 Correlations between the mean diameter of plasma EVs and circulating concentrations with clinical outputs in the whole cohort (n=45 women).

	Mean EVs diameter (nm)		**EVs/ml plasma**	
Correlations	**r**	**p**	**r**	**p**
Age (years)	-0.263	0.088	0.106	0.498
BMI (kg/m^2)	-0.525	**<0.001**	0.118	0.441
Fat mass (%)	-0.238	0.213	-0.179	0.353
Waist (cm)	-0.43	**0.014**	-0.31	0.085
Hip (cm)	-0.249	0.169	-0.18	0.323
WtH ratio	-0.308	0.081	-0.194	0.28
SBP (mm Hg)	-0.116	0.476	0.018	0.912
DBP (mm Hg)	-0.24	0.137	-0.155	0.341
Fasting glucose (mg/dl)	0.014	0.93	0.506	**<0.001**
Insulin (µIU/ml)	-0.397	**0.007**	0.042	0.783
HOMA-IR	-0.333	**0.031**	0.289	0.063
Glycated haemoglobin (%)	-0.039	0.811	0.322	**0.042**
Cholesterol (mg/dl)	-0.114	0.473	-0.13	0.413
HDL Cholesterol (mg/dl)	0.388	**0.011**	-0.225	0.152
LDL Cholesterol (mg/dl)	-0.172	0.275	-0.071	0.657
Triglycerides (mg/dl)	-0.444	**0.003**	0.125	0.43
EVs/ml plasma	0.009	0.955		

BMI: Body mass index, **WtH:** Waist to hip, **SBP:** Systolic blood pressure, **DBP:** Diastolic blood pressure, **HOMA-IR:** Homeostatic model assessment of insulin resistance, **HDL:** High-density lipoprotein, **LDL:** Low-density lipoprotein, **EVs:** Extracellular vesicles. Significant differences (Spearman's p-value < 0.05) are shown in **bold**.

Table 3 Partial correlations between miRNAs assessed in plasma EVs and paired-plasma samples and clinical outputs (n=45 women).

Spearman's Rho	BMI (kg/m^2)	Fasting glucose (mg/dl)	Fasting insulin (µIU/l)	HOMA-IR	CRP (mg/l)	Triglycerides (mg/dl)	Cholesterol (mg/dl)
miR-320a-3p EVs	**0.523 (0.001)**	0.143 (0.386)	0.097 (0.584)	0.066 (0.716)	0.122 (0.546)	0.062 (0.715)	**0.348 (0.035)**
miR-186-3p EVs	**-0.402 (0.011)**	0.208 (0.204)	-0.138 (0.437)	-0.026 (0.884)	**-0.475 (0.011)**	0.201 (0.233)	0.004 (0.982)
miR-892b EVs	**0.392 (0.012)**	-0.253 (0.115)	0.031 (0.858)	0.024 (0.893)	0.044 (0.822)	0.134 (0.422)	0.242 (0.144)
miR-106a-5p EVs	**0.381 (0.015)**	-0.21 (0.194)	0.029 (0.868)	-0.055 (0.759)	0.203 (0.301)	0.057 (0.736)	0.254 (0.125)
let-7b-5p EVs	**0.363 (0.023)**	-0.07 (0.672)	0.060 (0.737)	0.044 (0.81)	-0.026 (0.898)	0.06 (0.725)	0.096 (0.574)
miR-186-5p EVs	**-0.342 (0.031)**	0.150 (0.354)	-0.135 (0.438)	-0.127 (0.474)	**-0.490 (0.008)**	0.164 (0.324)	-0.115 (0.492)
miR-146a-5p EVs	**-0.343 (0.032)**	0.244 (0.135)	0.035 (0.843)	0.183 (0.309)	-0.331 (0.086)	0.032 (0.849)	-0.237 (0.159)
miR-323a-3p EVs	**0.317 (0.047)**	-0.138 (0.396)	0.024 (0.889)	-0.059 (0.739)	0.126 (0.522)	-0.092 (0.584)	0.198 (0.233)
miR-26b-5p EVs	0.35 (0.05)	0.175 (0.338)	**0.419 (0.029)**	**0.428 (0.026)**	0.203 (0.353)	0.280 (0.127)	0.097 (0.603)
miR-338-5p EVs	0.309 (0.053)	**-0.319 (0.045)**	0.022 (0.898)	-0.004 (0.983)	-0.034 (0.863)	0.044 (0.791)	0.206 (0.215)
miR-222-3p EVs	0.28 (0.089)	0.13 (0.437)	**0.357 (0.041)**	0.315 (0.079)	-0.02 (0.924)	-0.01 (0.954)	0.072 (0.675)
miR-212-3p EVs	0.214 (0.184)	-0.149 (0.36)	-0.111 (0.525)	-0.243 (0.166)	0.292 (0.132)	0.11 (0.513)	**0.416 (0.009)**
miR-30a-5p EVs	0.193 (0.233)	**-0.337 (0.034)**	0.001 (0.998)	-0.043 (0.81)	-0.153 (0.438)	-0.029 (0.861)	0.136 (0.416)
miR-342-3p EVs	0.183 (0.258)	-0.15 (0.357)	0.069 (0.693)	0.047 (0.794)	0.116 (0.556)	**-0.339 (0.037)**	-0.111 (0.507)
miR-150-5p EVs	0.151 (0.352)	-0.089 (0.586)	-0.113 (0.517)	-0.072 (0.687)	**0.407 (0.032)**	-0.101 (0.545)	0.116 (0.488)
miR-374a-5p EVs	-0.124 (0.46)	-0.133 (0.428)	-0.01 (0.956)	-0.039 (0.83)	0.144 (0.481)	**-0.476 (0.003)**	-0.1 (0.564)
miR-29c-3p EVs	0.06 (0.736)	0.019 (0.916)	-0.083 (0.661)	-0.183 (0.342)	0.232 (0.286)	0.309 (0.086)	**0.535 (0.002)**
miR-27a-3p EVs	-0.036 (0.826)	-0.289 (0.07)	-0.082 (0.642)	-0.052 (0.769)	**-0.432 (0.022)**	-0.05 (0.765)	-0.026 (0.876)
miR-223-3p EVs	-0.029 (0.86)	0.114 (0.485)	**0.346 (0.041)**	**0.427 (0.012)**	**-0.404 (0.033)**	0.023 (0.893)	-0.02 (0.906)
miR-320a-3p Plasma	0.245 (0.144)	0.076 (0.654)	0.123 (0.496)	0.133 (0.46)	-0.168 (0.367)	-0.069 (0.695)	0.201 (0.248)
miR-186-3p Plasma	-0.291 (0.069)	0.18 (0.266)	-0.323 (0.055)	-0.27 (0.111)	-0.271 (0.133)	0.231 (0.163)	**0.384 (0.017)**
miR-892b Plasma	0.194 (0.243)	0.24 (0.147)	0.1 (0.575)	0.106 (0.55)	-0.103 (0.576)	0.321 (0.056)	0.218 (0.202)
miR-106a-5p Plasma	-0.103 (0.538)	0.148 (0.375)	-0.076 (0.67)	-0.064 (0.72)	-0.27 (0.135)	0.245 (0.15)	**0.342 (0.041)**
let-7b-5p Plasma	-0.052 (0.76)	-0.158 (0.351)	-0.002 (0.99)	-0.032 (0.86)	-0.306 (0.101)	-0.203 (0.241)	-0.333 (0.051)
miR-186-5p Plasma	-0.293 (0.067)	0.041 (0.802)	-0.196 (0.252)	-0.197 (0.251)	**-0.393 (0.026)**	0.029 (0.863)	0.08 (0.634)
miR-146a-5p Plasma	0.082 (0.615)	0.116 (0.476)	-0.144 (0.402)	-0.109 (0.525)	-0.239 (0.188)	0.166 (0.319)	**0.4 (0.013)**
miR-323a-3p Plasma	0.209 (0.208)	0.082 (0.626)	0.011 (0.949)	0.021 (0.908)	-0.074 (0.688)	-0.049 (0.779)	-0.016 (0.928)
miR-26b-5p Plasma	-0.185 (0.26)	-0.051 (0.757)	-0.268 (0.12)	-0.241 (0.162)	-0.083 (0.653)	-0.183 (0.278)	-0.102 (0.547)
miR-338-5p Plasma	0.146 (0.382)	0.115 (0.491)	0.039 (0.828)	0.018 (0.92)	-0.152 (0.406)	0.266 (0.117)	0.142 (0.409)
miR-222-3p Plasma	-0.136 (0.401)	-0.144 (0.376)	-0.152 (0.376)	-0.123 (0.476)	-0.059 (0.749)	-0.089 (0.596)	0.012 (0.941)
miR-212-3p Plasma	-0.106 (0.525)	-0.222 (0.18)	**-0.449 (0.008)**	**-0.455 (0.007)**	-0.127 (0.487)	0.086 (0.62)	0.214 (0.209)
miR-30a-5p Plasma	-0.108 (0.512)	-0.297 (0.066)	-0.290 (0.091)	-0.323 (0.059)	-0.042 (0.819)	-0.163 (0.336)	0.046 (0.786)
miR-342-3p Plasma	0.206 (0.209)	0.197 (0.229)	0.155 (0.373)	0.271 (0.115)	0.224 (0.217)	0.143 (0.399)	0.106 (0.534)
miR-150-5p Plasma	0.223 (0.172)	0.225 (0.169)	0.171 (0.327)	0.186 (0.284)	0.029 (0.873)	0.071 (0.678)	-0.032 (0.85)
miR-374a-5p Plasma	-0.092 (0.576)	0.21 (0.2)	0.072 (0.679)	0.131 (0.453)	0.018 (0.92)	0.006 (0.973)	-0.175 (0.3)
miR-29c-3p Plasma	**-0.326 (0.049)**	-0.005 (0.979)	-0.237 (0.184)	-0.255 (0.152)	-0.291 (0.113)	-0.127 (0.467)	0.177 (0.308)
miR-27a-3p Plasma	-0.004 (0.982)	0.143 (0.38)	0.262 (0.122)	0.265 (0.118)	-0.116 (0.526)	0.318 (0.052)	**0.377 (0.019)**
miR-223-3p Plasma	-0.009 (0.955)	0.13 (0.425)	0.17 (0.322)	0.177 (0.301)	-0.081 (0.659)	0.016 (0.925)	0.135 (0.418)

BMI: Body mass index, **HOMA-IR:** Homeostatic model assessment of insulin resistance, **EVs:** Extracellular vesicles. Significant differences ($p<0.05$) are shown in **bold**.

REFERENCES

[1] Raposo G, Stoorvogel W. Extracellular vesicles: exosomes, microvesicles, and friends. J Cell Biol. 2013;200:373-83.

[2] Arraud N, Linares R, Tan S, Gounou C, Pasquet JM, Mornet S, et al. Extracellular vesicles from blood plasma: determination of their morphology, size, phenotype and concentration. J Thromb Haemost. 2014;12:614-27.

[3] Han WQ, Chang FJ, Wang QR, Pan JQ. Microparticles from Patients with the Acute Coronary Syndrome Impair Vasodilatation by Inhibiting the Akt/eNOS-Hsp90 Signaling Pathway. Cardiology. 2015;132:252-60.

[4] Kranendonk ME, de Kleijn DP, Kalkhoven E, Kanhai DA, Uiterwaal CS, van der Graaf Y, et al. Extracellular vesicle markers in relation to obesity and metabolic complications in patients with manifest cardiovascular disease. Cardiovasc Diabetol. 2014;13:37.

[5] Agouni A, Lagrue-Lak-Hal AH, Ducluzeau PH, Mostefai HA, Draunet-Busson C, Leftheriotis G, et al. Endothelial dysfunction caused by circulating microparticles from patients with metabolic syndrome. Am J Pathol. 2008;173:1210-9.

[6] Mleczko J, Ortega FJ, Falcon-Perez JM, Wabitsch M, Fernandez-Real JM, Mora S. Extracellular Vesicles from Hypoxic Adipocytes and obese subjects reduce Insulin-Stimulated Glucose Uptake. Mol Nutr Food Res. 2018.

[7] Bonora E, Targher G, Alberiche M, Bonadonna RC, Saggiani F, Zenere MB, et al. Homeostasis model assessment closely mirrors the glucose clamp technique in the assessment of insulin sensitivity: studies in subjects with various degrees of glucose tolerance and insulin sensitivity. Diabetes Care. 2000;23:57-63.

[8] Thery C, Amigorena S, Raposo G, Clayton A. Isolation and characterization of exosomes from cell culture supernatants and biological fluids. Curr Protoc Cell Biol. 2006;Chapter 3:Unit 3 22.

[9] Filipe V, Hawe A, Jiskoot W. Critical evaluation of Nanoparticle Tracking Analysis (NTA) by NanoSight for the measurement of nanoparticles and protein aggregates. Pharm Res. 2010;27:796-810.

[10] Vestad B, Llorente A, Neurauter A, Phuyal S, Kierulf B, Kierulf P, et al. Size and concentration analyses of extracellular vesicles by nanoparticle tracking analysis: a variation study. J Extracell Vesicles. 2017;6:1344087.

[11] Ortega FJ, Mercader JM, Catalan V, Moreno-Navarrete JM, Pueyo N, Sabater M, et al. Targeting the circulating microRNA signature of obesity. Clin Chem. 2013;59:781-92.

[12] Ortega FJ, Moreno M, Mercader JM, Moreno-Navarrete JM, Fuentes-Batllevell N, Sabater M, et al. Inflammation triggers specific microRNA profiles in human adipocytes and macrophages and in their supernatants. Clin Epigenetics. 2015;7:49.

[13] Mar JC, Kimura Y, Schroder K, Irvine KM, Hayashizaki Y, Suzuki H, et al. Data-driven normalization strategies for high-throughput quantitative RT-PCR. BMC Bioinformatics. 2009;10:110.

[14] Vandesompele J, De Preter K, Pattyn F, Poppe B, Van Roy N, De Paepe A, et al. Accurate normalization of real-time quantitative RT-PCR data by geometric averaging of multiple internal control genes. Genome Biol. 2002;3:RESEARCH0034.

[15] Ortega FJ, Mercader JM, Catalan V, Moreno-Navarrete JM, Pueyo N, Sabater M, et al. Targeting the Circulating MicroRNA Signature of Obesity. Clin Chem.

591 [16] Zhang J, Tang H, Zhang Y, Deng R, Shao L, Liu Y, et al. Identification of suitable
592 reference genes for quantitative RT-PCR during 3T3-L1 adipocyte differentiation. Int J
593 Mol Med. 2014;33:1209-18.
594 [17] Bolukbasi MF, Mizrak A, Ozdener GB, Madlener S, Strobel T, Erkan EP, et al.
595 miR-1289 and "Zipcode"-like Sequence Enrich mRNAs in Microvesicles. Mol Ther
596 Nucleic Acids. 2012;1:e10.
597 [18] Ludwig N, Leidinger P, Becker K, Backes C, Fehlmann T, Pallasch C, et al.
598 Distribution of miRNA expression across human tissues. Nucleic Acids Res.
599 2016;44:3865-77.
600 [19] Guay C, Regazzi R. Exosomes as new players in metabolic organ cross-talk.
601 Diabetes Obes Metab. 2017;19 Suppl 1:137-46.
602 [20] van Niel G, D'Angelo G, Raposo G. Shedding light on the cell biology of
603 extracellular vesicles. Nat Rev Mol Cell Biol. 2018.
604 [21] Thomou T, Mori MA, Dreyfuss JM, Konishi M, Sakaguchi M, Wolfrum C, et al.
605 Adipose-derived circulating miRNAs regulate gene expression in other tissues. Nature.
606 2017;542:450-5.
607 [22] Osada-Oka M, Shiota M, Izumi Y, Nishiyama M, Tanaka M, Yamaguchi T, et al.
608 Macrophage-derived exosomes induce inflammatory factors in endothelial cells under
609 hypertensive conditions. Hypertens Res. 2016;40:353-60.
610 [23] Eirin A, Riester SM, Zhu XY, Tang H, Evans JM, O'Brien D, et al. MicroRNA and
611 mRNA cargo of extracellular vesicles from porcine adipose tissue-derived
612 mesenchymal stem cells. Gene. 2014;551:55-64.
613 [24] Phinney DG, Di Giuseppe M, Njah J, Sala E, Shiva S, St Croix CM, et al.
614 Mesenchymal stem cells use extracellular vesicles to outsource mitophagy and shuttle
615 microRNAs. Nat Commun. 2015;6:8472.
616 [25] Muller G, Schneider M, Biemer-Daub G, Wied S. Microvesicles released from rat
617 adipocytes and harboring glycosylphosphatidylinositol-anchored proteins transfer RNA
618 stimulating lipid synthesis. Cell Signal. 2011;23:1207-23.
619 [26] Muller G, Schneider M, Biemer-Daub G, Wied S. Upregulation of lipid synthesis
620 in small rat adipocytes by microvesicle-associated CD73 from large adipocytes. Obesity
621 (Silver Spring). 2011;19:1531-44.
622 [27] Phoonsawat W, Aoki-Yoshida A, Tsuruta T, Sonoyama K. Adiponectin is partially
623 associated with exosomes in mouse serum. Biochem Biophys Res Commun.
624 2014;448:261-6.
625 [28] Durcin M, Fleury A, Taillebois E, Hilairet G, Krupova Z, Henry C, et al.
626 Characterisation of adipocyte-derived extracellular vesicle subtypes identifies distinct
627 protein and lipid signatures for large and small extracellular vesicles. J Extracell
628 Vesicles. 2017;6:1305677.
629 [29] Stepanian A, Bourguignat L, Hennou S, Coupaye M, Hajage D, Salomon L, et al.
630 Microparticle increase in severe obesity: not related to metabolic syndrome and
631 unchanged after massive weight loss. Obesity (Silver Spring). 2013;21:2236-43.
632 [30] Davidson SM, Riquelme JA, Takov K, Vicencio JM, Boi-Doku C, Khoo V, et al.
633 Cardioprotection mediated by exosomes is impaired in the setting of type II diabetes but
634 can be rescued by the use of non-diabetic exosomes in vitro. J Cell Mol Med. 2017.
635 [31] Salomon C, Scholz-Romero K, Sarker S, Sweeney E, Kobayashi M, Correa P, et al.
636 Gestational Diabetes Mellitus Is Associated With Changes in the Concentration and
637 Bioactivity of Placenta-Derived Exosomes in Maternal Circulation Across Gestation.
638 Diabetes. 2016;65:598-609.
639 [32] Santovito D, De Nardis V, Marcantonio P, Mandolini C, Paganelli C, Vitale E, et
640 al. Plasma exosome microRNA profiling unravels a new potential modulator of

641 adiponectin pathway in diabetes: effect of glycemic control. J Clin Endocrinol Metab.
642 2014;99:E1681-5.
643 [33] Hulsmans M, Holvoet P. MicroRNA-containing microvesicles regulating
644 inflammation in association with atherosclerotic disease. Cardiovasc Res. 2013;100:7-
645 18.
646 [34] Jansen F, Yang X, Hoelscher M, Cattelan A, Schmitz T, Proebsting S, et al.
647 Endothelial microparticle-mediated transfer of MicroRNA-126 promotes vascular
648 endothelial cell repair via SPRED1 and is abrogated in glucose-damaged endothelial
649 microparticles. Circulation. 2013;128:2026-38.
650 [35] Ren J, Zhang J, Xu N, Han G, Geng Q, Song J, et al. Signature of circulating
651 microRNAs as potential biomarkers in vulnerable coronary artery disease. PLoS One.
652 2013;8:e80738.
653 [36] Martinez MC, Andriantsitohaina R. Extracellular Vesicles in Metabolic Syndrome.
654 Circ Res. 2017;120:1674-86.
655 [37] Zhang Y, Yu M, Tian W. Physiological and pathological impact of exosomes of
656 adipose tissue. Cell Prolif. 2016;49:3-13.
657
658
659

FIGURES LEGEND

Figure 1 A. Microscopic analysis of the morphology of isolated plasma EVs using TEM and negative staining. **B.** NTA particle concentration according to the particle size in lean (BMI< 25 kg/m^2), overweight (25≤ BMI< 30 kg/m^2), and obese (30≤ BMI< 35 kg/m^2; and BMI≥ 35 kg/m^2) women. **C.** Mean and 95% confidence interval for circulating EVs in each subgroup. **D.** Association between BMI and EVs size, and **E.** between fasting glucose and the concentrations of EVs found in plasma of lean (empty circles), overweight (diamonds), and obese participants with BMI of 30-35 kg/m^2 (straight triangles), and ≥35 kg/m^2 (inverted triangles).

Figure 2 Indexes of correlation between miRNAs found in EVs and paired plasma samples and parameters of interest. **BMI**: Body mass index, **HOMA-IR**: Homeostatic model assessment of insulin resistance, **HbA1C**: Glycated haemoglobin, **HDL**: High-density lipoprotein, **LDL**: Low-density lipoprotein, **CRP**: C reactive protein, **EVs**: Extracellular vesicles (size or numbers).

Figure 3 Gene expression measures obtained in undifferentiated (PA) and differentiated mature adipocytes (MA) upon treatment with macrophage LPS-conditioned media (MCM) and plasma EVs isolated from 12 participants, grouped in “Lean” or “Obese” EVs according to the donors’ BMI. Three biological replicates were performed for each treatment.

Figure 1

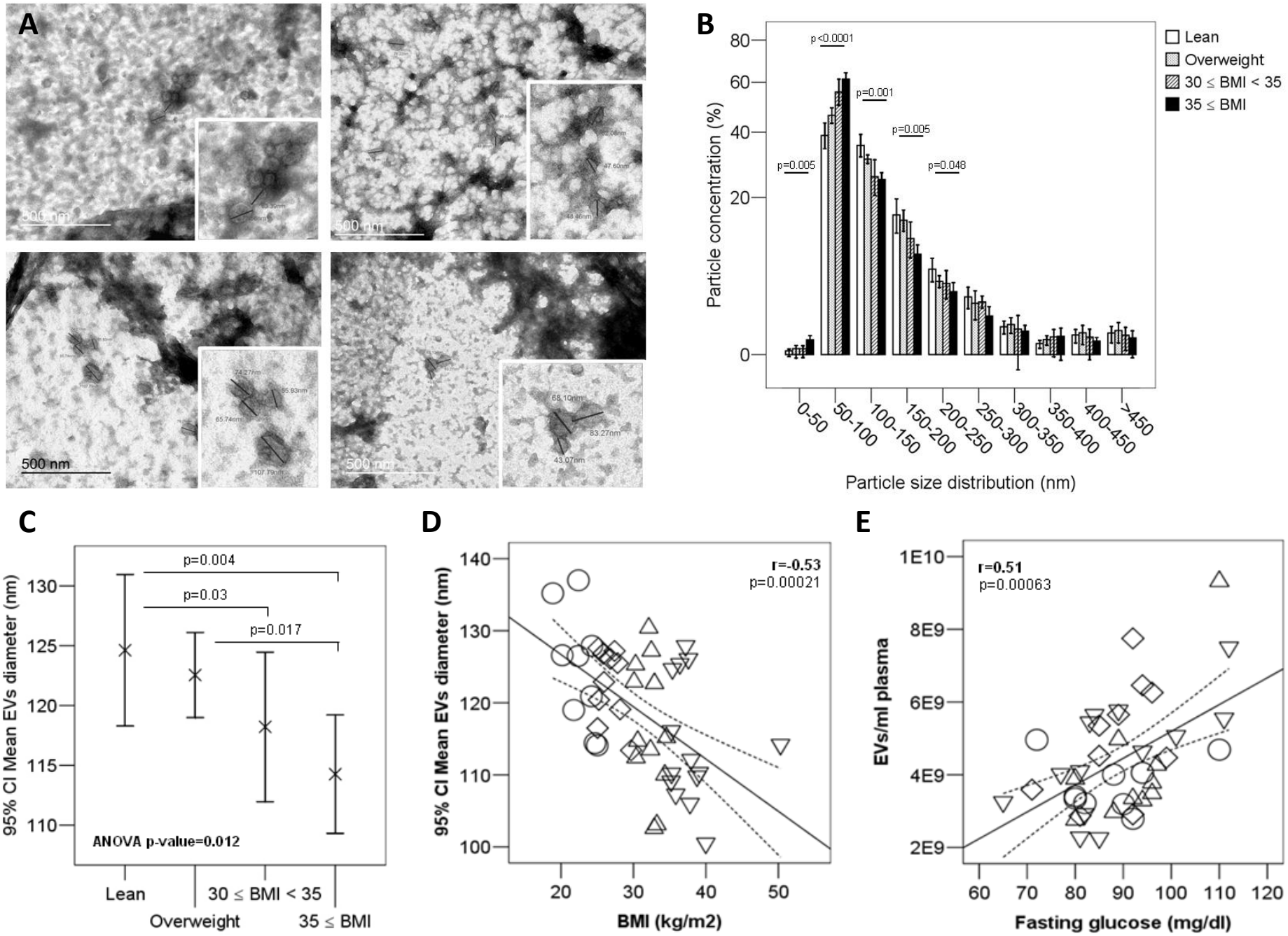
A
500 nm
B
Lean
Overweight
30 ≤ BMI < 35
35 ≤ BMI
p<0.0001
p=0.001
p=0.005
p=0.005
p=0.048
Particle concentration (%)
0
20
40
60
80
0-50
50-100
100-150
150-200
200-250
250-300
300-350
350-400
400-450
>450
Particle size distribution (nm)
C
p=0.004
p=0.03
p=0.017
95% CI Mean EVs diameter (nm)
110
115
120
125
130
ANOVA p-value=0.012
Lean
30 ≤ BMI < 35
Overweight
35 ≤ BMI
D
r=-0.53
p=0.00021
95% CI Mean EVs diameter (nm)
100
110
120
130
140
20
30
40
50
BMI (kg/m2)
E
r=0.51
p=0.00063
EVs/ml plasma
2E9
4E9
6E9
8E9
1E10
60
70
80
90
100
110
120
Fasting glucose (mg/dl)

Figure 2

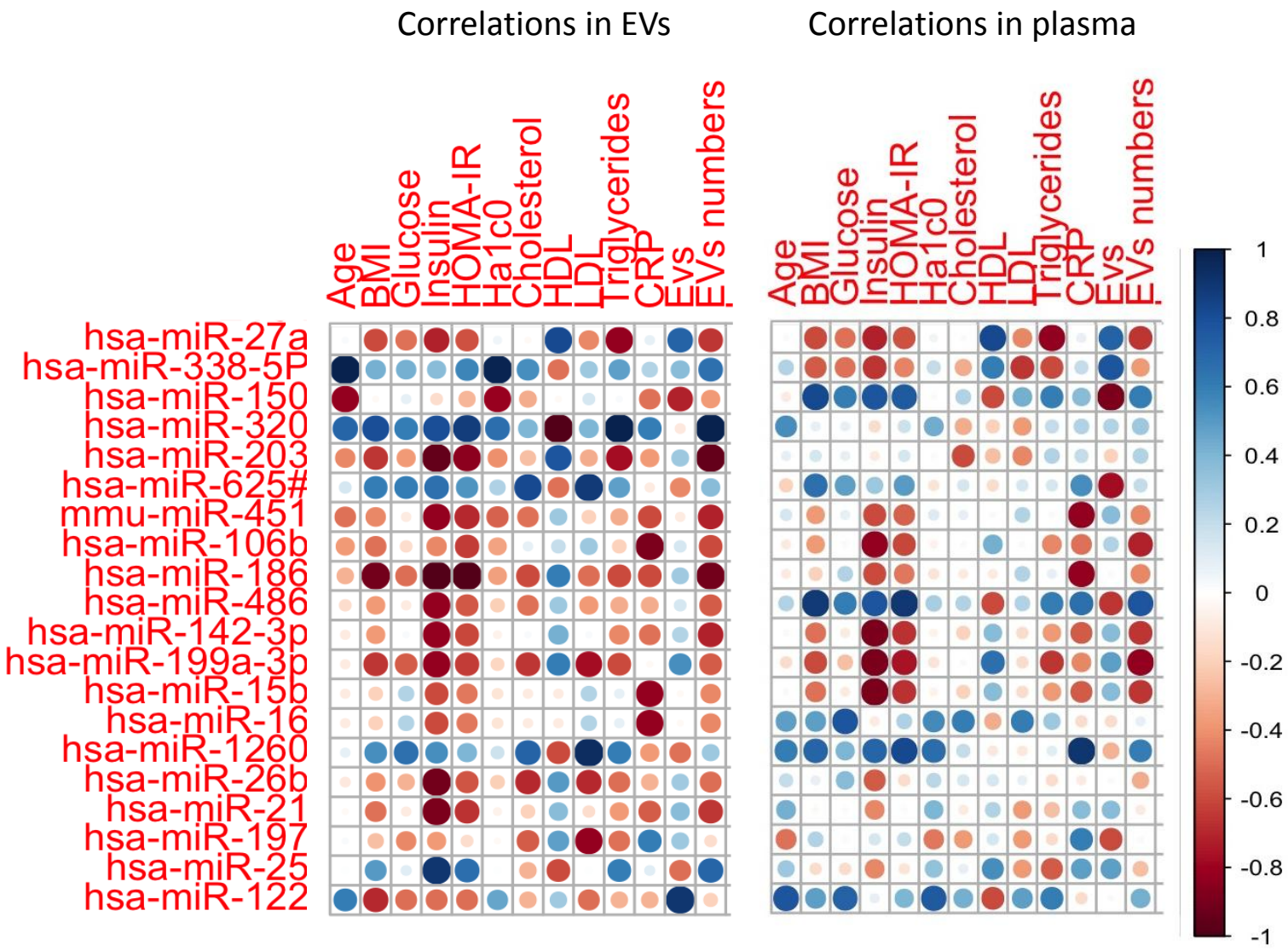
Correlations in EVs
Correlations in plasma
Age
BMI
Glucose
Insulin
HOMA-IR
Ha1c0
Cholesterol
HDL
LDL
Triglycerides
CRP
Evs
EVs numbers
hsa-miR-27a
hsa-miR-338-5P
hsa-miR-150
hsa-miR-320
hsa-miR-203
hsa-miR-625#
mmu-miR-451
hsa-miR-106b
hsa-miR-186
hsa-miR-486
hsa-miR-142-3p
hsa-miR-199a-3p
hsa-miR-15b
hsa-miR-16
hsa-miR-1260
hsa-miR-26b
hsa-miR-21
hsa-miR-197
hsa-miR-25
hsa-miR-122
1
0.8
0.6
0.4
0.2
0
-0.2
-0.4
-0.6
-0.8
-1

Figure 3

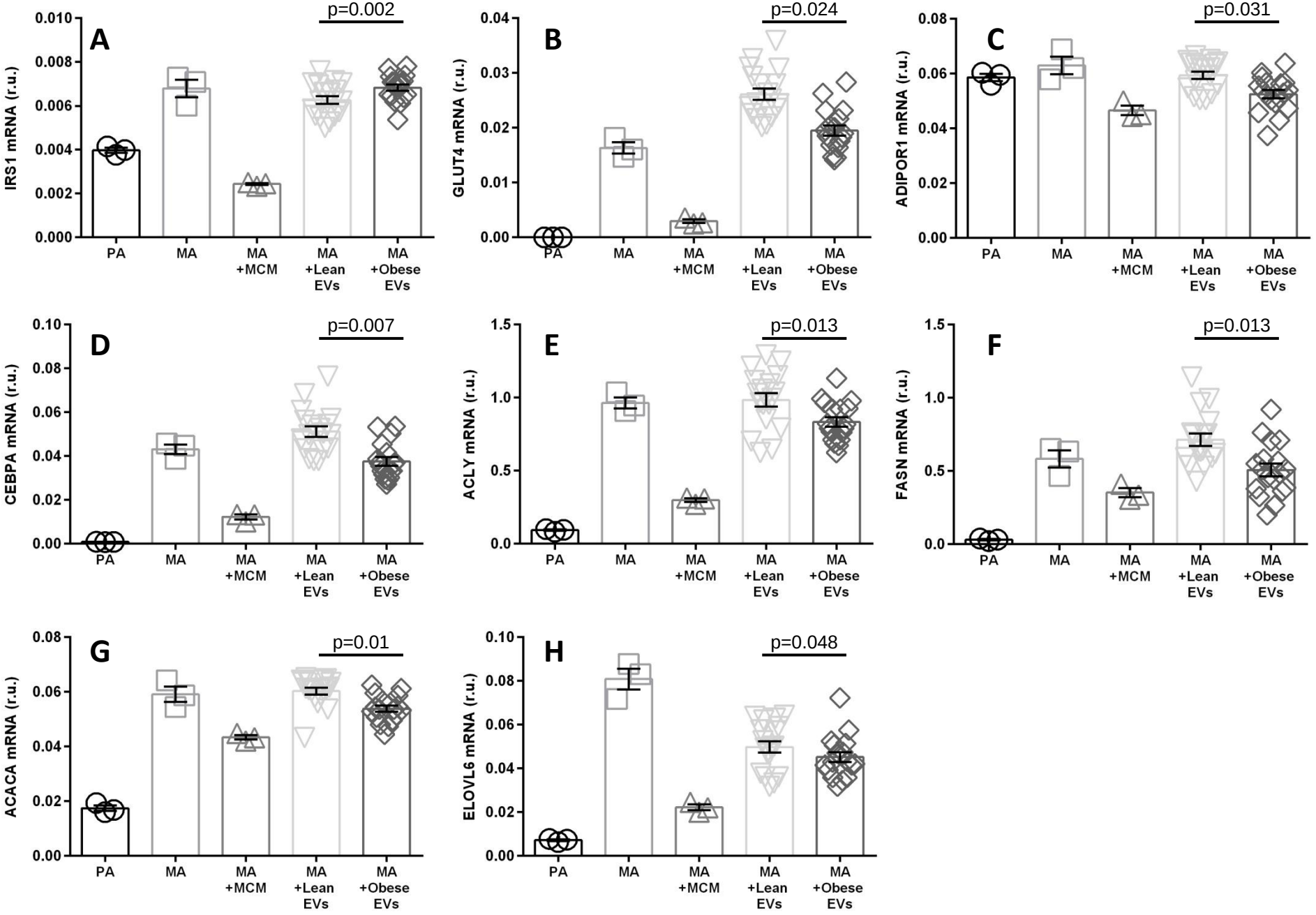
A
p=0.002
IRS1 mRNA (r.u.)
0.010
0.008
0.006
0.004
0.002
0.000
B
p=0.024
GLUT4 mRNA (r.u.)
0.04
0.03
0.02
0.01
0.00
C
p=0.031
ADIPOR1 mRNA (r.u.)
0.08
0.06
0.04
0.02
0.00
D
p=0.007
CEBPA mRNA (r.u.)
0.10
0.08
0.06
0.04
0.02
0.00
E
p=0.013
ACLY mRNA (r.u.)
1.5
1.0
0.5
0.0
F
p=0.013
FASN mRNA (r.u.)
1.5
1.0
0.5
0.0
G
p=0.01
ACACA mRNA (r.u.)
0.08
0.06
0.04
0.02
0.00
H
p=0.048
ELOVL6 mRNA (r.u.)
0.10
0.08
0.06
0.04
0.02
0.00
PA
MA
MA +MCM
MA +Lean EVs
MA +Obese EVs

Supplemental Table 1 Mean ± standard deviation for anthropometrical and biochemical parameters in women preselected for sample pooling, merge and miRNA profiling in plasma and isolated plasma EVs. Each column reports mean values of 3 subjects, so the assessment included samples from 18 participants.

Pools	**Lean #1**	**Lean #2**	**Lean #3**	**Obese #1**	**Obese #2**	**Obese #3**	**Student t-test**
Age (years)	39 ± 16	40 ± 13	36 ± 6	44 ± 8	35 ± 2	45 ± 1	0.658
BMI (kg/m^2)	21.6 ± 2.7	22.4 ± 2.3	24.8 ± 0.4	36.9 ± 0.9	36.4 ± 2	40.7 ± 8.4	**<0.0001**
Fat mass (%)	22.1 ± 2.7	19.2 ± 6.9	23.7 ± 1.2	55 ± 0.2	65.9 ± 0.7	34.2 ± 8.2	**<0.0001**
Waist (cm)	81.3 ± 3.2	78.3 ± 5.3	85 ± 1.4	100.3 ± 1.8	98.0 ± 1.9	95.5 ± 9.2	**<0.0001**
Hip (cm)	92.5 ± 4.9	90.3 ± 1.8	95.3 ± 3.2	115 ± 3.5	112.0 ± 4.5	111.3 ± 3.2	**<0.0001**
WtH ratio	0.88 ± 0.01	0.87 ± 0.04	0.89 ± 0.04	0.87 ± 0.04	0.88 ± 0.12	0.86 ± 0.11	0.681
SBP (mm Hg)	128.5 ± 17.7	148.5 ± 60.1	104 ± 4.2	126.5 ± 4.9	125.3 ± 4.5	125.5 ± 6.4	0.931
DBP (mm Hg)	72 ± 4.2	80.5 ± 23.3	73 ± 1.4	80.5 ± 2.1	76.3 ± 5.5	76.7 ± 4.7	0.608
Fasting glucose (mg/dl)	83.3 ± 4.2	80.7 ± 9	89 ± 7	96.3 ± 13.7	84.0 ± 4.4	99.3 ± 13.6	0.076
Insulin (µIU/ml)	3.5 ± 1.3	6.8 ± 2.6	4.2 ± 2.1	7.8 ± 3.3	7.5 ± 1.7	7.4 ± 2.6	**0.022**
HOMA-IR	0.7 ± 0.24	1.39 ± 0.61	0.90 ± 0.36	1.92 ± 1.01	1.56 ± 0.35	1.87 ± 0.83	**0.013**
Glycated haemoglobin (%)	4.5 ± 0.7	4.8 ± 0.3	4.5 ± 0.5	5.4 ± 0.4	4.4 ± 0.3	5.3 ± 0.6	0.08
Cholesterol (mg/dl)	175.3 ± 11	190.3 ± 38	218.7 ± 32.3	228.3 ± 26.7	182 ± 35	195.7 ± 14.2	0.633
HDL Cholesterol (mg/dl)	66.7 ± 14.7	91.5 ± 18.7	67.7 ± 12.3	48.7 ± 11.3	54.6 ± 10.4	53.7 ± 12.4	**0.004**
LDL Cholesterol (mg/dl)	92.7 ± 20.8	89.9 ± 27.5	135.9 ± 35.7	160.5 ± 22.6	110.5 ± 34.1	123.1 ± 16.4	0.119
Triglycerides (mg/dl)	79.7 ± 23.4	43 ± 15.6	75.3 ± 7.5	96.3 ± 52.3	84.7 ± 35.2	94.0 ± 34.7	0.095
CRP (mg/dl)	0.21 ± 0.16	1.36 ± 1.84	0.35 ± 0.07	0.47 ± 0.37	0.60 ± 0.45	0.85 ± 0.78	0.91
Mean EVs diameter (nm)	125 ± 8.9	126 ± 11.3	119.5 ± 7.4	120.4 ± 11.4	114.5 ± 8.8	116.6 ± 7.9	0.139
EVs/ml plasma (x 10^6)	3,545 ± 409	3,831 ± 980	3,238 ± 707	5,279 ± 556	4,263 ± 1,432	4,944 ± 2623	**0.04**

BMI: Body mass index, **WtH:** Waist to hip ratio, **SBP:** Systolic blood pressure, **DBP:** Diastolic blood pressure, **HOMA-IR:** Homeostatic model assessment of insulin resistance, **HDL:** High-density lipoprotein, **LDL:** Low-density lipoprotein, **EVs:** Extracellular vesicles. Significant differences ($p<0.05$) between lean and obese groups are shown in **bold**.

Supplemental Table 2 List of commercially available TaqMan® Gene Expression and MicroRNA assays used in this study.

Genes	**Assay ID#**	**MicroRNAs**	**Assay ID#**
Inflammation		hsa-let-7b-5p	2619
IL6	Hs00985639_m1	hsa-miR-106a-5p	2169
IL8	Hs00174103_m1	hsa-miR-106b-5p	442
Insulin pathway		hsa-miR-122-5p	2245
GLUT4	Hs00168966_m1	hsa-miR-143-3p	2249
IRS1	Hs00178563_m1	hsa-miR-145-5p	2278
PI3KR	Hs00933163_m1	hsa-miR-146a-5p	468
Adipogenesis		hsa-miR-146b-5p	1097
SREBF1	Hs01088679_g1	hsa-miR-150-5p	473
CEBPA	Hs00269972_s1	hsa-miR-155-5p	2623
ADIPOQ	Hs00605917_m1	hsa-miR-186-3p	2105
ADIPOR1	Hs00360422_m1	hsa-miR-186-5p	2285
Lipogenesis		hsa-miR-194-5p	493
ACLY	Hs00982738_m1	hsa-miR-212-3p	515
ACACA	Hs01046047_m1	hsa-miR-222-3p	2276
FASN	Hs01005622_m1	hsa-miR-223-3p	2295
ELOVL6	Hs00907564_m1	hsa-miR-26b-5p	407
Lipolysis		hsa-miR-27a-3p	408
AQP9	Hs01033361_m1	hsa-miR-29c-3p	587
Type II diabetes		hsa-miR-30a-5p	417
ADIPOR2	Hs00226105_m1	hsa-miR-301a-3p	528
Fatty Acid alpha oxidation		hsa-miR-320a-3p	2277
PTGS2	Hs00153133_m1	hsa-miR-323a-3p	2227
HMGB1 pathway		hsa-miR-331-3p	545
CXCL8	Hs00174103_m	hsa-miR-338-5p	2658
IGF1-signaling		hsa-miR-342-3p	2260
STAT3	Hs00374280_m1	hsa-miR-374a-5p	563
Insulin receptor; Leptin Signaling in obesity		hsa-miR-892b	2214
PDE3B	Hs00265322_m1	**Housekeeping**	
Housekeeping		hsa-miR-30c-5p	419
PPIA	Hs99999904_m1	hsa-miR-24-3p	402
		hsa-miR-484	1821

IL6 and **8:** Interleukin 6 and 8, **GLUT4:** Solute carrier family 2 (facilitated glucose transporter), member 4, **IRS1:** Insulin receptor substrate 1, **PI3KR:** Phosphoinositide-3-kinase regulatory subunit 1, **SREBF1:** Sterol regulatory element binding transcription factor 1, **CEBPA:** CCAAT/enhancer binding protein alpha, **ADIPOQ:** Adiponectin, **ADIPOR1:** Adiponectin receptor 1, **ACLY:** ATP citrate lyase, **ACACA:** Acetyl-CoA carboxylase alpha, **FASN:** Fatty acid synthase, **ELOVL6:** ELOVL fatty acid elongase 6, **AQP9:** Aquaporin 9, **ADIPOR2:** Adiponectin receptor 2, **PTGS2:** Prostaglandin-endoperoxide synthase 2, **CXCL8:** C-X-C motif chemokine ligand 8, **STAT3:** Signal transducer and activator of transcription 3, **PDE3B:** Phosphodiesterase 3B, **PPIA:** Peptidylprolyl isomerase A.

Supplemental Table 3 Nominal variations found in plasma and plasma-derived EVs-contained miRNAs of obese (BMI≥35 kg/m^2) vs. lean (BMI<25 kg/m^2) women.

	Plasma EVs		**Plasma**	
miRNA – Assay ID#	**Fold change**	**p-value**	**Fold change**	**p-value**
hsa-miR-331 – 000545	-14.47	**0.0114**	1.05	0.875
hsa-miR-320 – 002277	4.74	**0.0119**	1.65	0.265
hsa-miR-186 – 002285	-7.73	**0.0167**	1.57	0.424
hsa-miR-30a-5p – 000417	4.20	**0.0207**	-1.22	0.790
hsa-miR-16 – 000391	-4.68	**0.0225**	1.56	0.054
hsa-miR-141* – 002145	5.07	**0.0255**	1.33	0.34
hsa-miR-875-5p – 002203	5.11	**0.0279**	6.02	0.564
hsa-miR-376a – 000565	138.90	**0.0314**	2.51	0.147
hsa-miR-27a – 000408	-5.16	**0.0331**	-1.78	0.257
hsa-miR-618 – 001593	3.71	**0.0332**	-7.37	0.486
hsa-miR-15b – 000390	-3.07	**0.0339**	-1.53	0.224
hsa-miR-342-3p – 002260	-14.39	**0.0344**	2.99	0.317
U6-snRNA – 001973e	-5.38	**0.0421**	1.62	0.460
hsa-miR-25 – 000403	2101.61	**0.0467**	-1.84	0.324
hsa-miR-1290– 002863	7.74	**0.0475**	2.83	0.214
hsa-miR-432 – 001026	378.48	0.0635	1.62	0.377
hsa-miR-378 – 002243	2.22	0.0804	-2.06	0.319
hsa-miR-103 – 000439	-2.33	0.084	-1.78	0.257
hsa-miR-520D-3P – 002743	6.43	0.097	2.36	0.346
hsa-miR-892b – 002214	2.66	0.099	4.73	**0.027**

Supplemental Table 4 Association between clinical outputs (n=12 individuals, 6 lean and 6 obese women) and gene expression measures assessed in mature adipocytes after treatment with plasma EVs (~250,000 plasma EVs/µl, 24 h, 3 biological replicates/treatment).

	Age (y)	BMI (kg/m2)	Glucose (mg/dl)	Insulin (µIU/l)	HOMA-IR	HbA1c (%)
Inflammation						
IL6	r=-0.08 (0.638)	r=-0.197 (0.224)	**r=-0.357 (0.024)**	**r=-0.462 (0.003)**	**r=-0.459 (0.003)**	**r=-0.644 (<0.0001)**
IL8	**r=-0.424 (0.009)**	r=-0.220 (0.173)	**r=-0.569 (<0.0001)**	r=-0.175 (0.28)	r=-0.25 (0.12)	r=-0.317 (0.059)
Insulin pathway						
GLUT4	r=-0.042 (0.796)	**r=-0.471 (0.001)**	r=0.03 (0.85)	**r=0.358 (0.023)**	**r=0.497 (0.001)**	r=0.036 (0.826)
IRS1	r=0.288 (0.079)	**r=0.483 (0.001)**	r=-0.089 (0.582)	**r=0.356 (0.022)**	r=0.246 (0.121)	**r=0.359 (0.027)**
PI3KR	r=0.076 (0.643)	r=0.172 (0.265)	r=-0.221 (0.149)	r=-0.061 (0.695)	r=-0.073 (0.64)	r=-0.166 (0.307)
Adipogenesis						
SREBF1	r=0.230 (0.183)	r=-0.206 (0.214)	r=0.105 (0.531)	**r=-0.511 (0.001)**	**r=-0.408 (0.011)**	**r=-0.408 (0.015)**
CEBPA	r=-0.089 (0.621)	**r=-0.619 (<0.0001)**	r=0.13 (0.45)	r=-0.092 (0.593)	r=0.061 (0.725)	r=-0.141 (0.435)
ADIPOQ	**r=0.373 (0.030)**	r=-0.041 (0.808)	r=-0.083 (0.619)	r=-0.212 (0.201)	r=-0.18 (0.281)	r=-0.092 (0.598)
ADIPOR1	r=0.112 (0.514)	r=-0.291 (0.072)	r=0.188 (0.253)	r=-0.166 (0.314)	r=-0.073 (0.661)	r=-0.281 (0.097)
Lipogenesis						
ACLY	r=-0.034 (0.842)	**r=-0.391 (0.013)**	r=0.059 (0.716)	**r=-0.320 (0.044)**	r=-0.228 (0.157)	**r=-0.346 (0.039)**
ACACA	r=-0.143 (0.361)	**r=-0.373 (0.01)**	r=0.012 (0.936)	r=-0.041 (0.785)	r=0.005 (0.973)	r=-0.11 (0.481)
FASN	r=-0.332 (0.059)	**r=-0.550 (0.001)**	r=-0.150 (0.381)	**r=0.424 (0.014)**	**r=0.550 (0.001)**	r=-0.136 (0.452)
ELOVL6	r=-0.009 (0.952)	r=-0.277 (0.057)	r=-0.093 (0.531)	**r=-0.394 (0.006)**	**r=-0.341 (0.018)**	**r=-0.322 (0.033)**
Lipolysis						
AQP9	r=-0.188 (0.294)	r=-0.272 (0.109)	r=-0.104 (0.548)	r=-0.227 (0.184)	r=-0.189 (0.27)	**r=-0.496 (0.003)**
Type II diabetes						
ADIPOR2	r=0.226 (0.107)	r=0.031 (0.823)	**r=0.293 (0.028)**	**r=0.29 (0.03)**	**r=0.269 (0.045)**	**r=0.411 (0.002)**
Fatty Acid alpha oxidation						
PTGS2	r=0.092 (0.519)	r=-0.178 (0.193)	r=-0.029 (0.843)	r=-0.02 (0.887)	r=-0.007 (0.995)	**r=-0.317 (0.024)**
HMGB1 pathway						
CXCL8	**r=-0.34 (0.014)**	r=0.22 (0.106)	r=-0.15 (0.273)	r=0.128 (0.35)	r=0.088 (0.524)	r=0.149 (0.296)
IGF1-signaling						
STAT3	**r=0.283 (0.044)**	r=0.126 (0.362)	**r=0.39 (0.004)**	**r=0.313 (0.021)**	**r=0.295 (0.03)**	**r=0.416 (0.003)**
Insulin receptor; Leptin Signaling in obesity						
PDE3B	r=0.176 (0.212)	r=0.044 (0.746)	**r=0.3 (0.024)**	**r=0.284 (0.033)**	r=0.238 (0.078)	**r=0.37 (0.007)**

BMI: Body mass index, **HbA1c:** Glycated haemoglobin, **HOMA-IR:** Homeostatic model assessment of insulin resistance, **IL6** and **8:** Interleukin 6 and 8, **GLUT4:** Solute carrier family 2 (facilitated glucose transporter), member 4, **IRS1:** Insulin receptor substrate 1, **PI3KR:** Phosphoinositide-3-kinase regulatory subunit 1, **SREBF1:** Sterol regulatory element binding transcription factor 1, **CEBPA:** CCAAT/enhancer binding protein alpha, **ADIPOQ:** Adiponectin, **ADIPOR1:** Adiponectin receptor 1, **ACLY:** ATP citrate lyase, **ACACA:** Acetyl-CoA carboxylase alpha, **FASN:** Fatty acid synthase, **ELOVL6:** ELOVL fatty acid elongase 6, **AQP9:** Aquaporin 9, **ADIPOR2:** Adiponectin receptor 2, **PTGS2:** Prostaglandin-endoperoxide synthase 2, **CXCL8:** C-X-C motif chemokine ligand 8, **STAT3:** Signal transducer and activator of transcription 3, **PDE3B:** Phosphodiesterase 3B. Significant differences ($p<0.05$) are shown in **bold**.

Supplemental Table 5 Genes involved in metabolism with seeding sequences reported and empirically validated for miRNAs found in plasma EVs.

Gene	Canonical Pathway	# of miRNAs in obese EVs	# of miRNAs in lean EVs	miRNAs
PTGS2	Fatty Acid alpha oxidation	3	1	miR-155-5p, let-7b-5p, miR-146a/b-5p
ADIPOR2	Type II diabetes	2	0	let-7b-5p, miR-892b
CXCL8	HMGB1	4	1	miR-155-5p, let-7b-5p, miR-106a-5p, miR-146a/b-5p
STAT3	IGF1-signaling	3	1	miR-155-5p, let-7b-5p, miR-106a-5p, miR-301a-3p
PDE3B	Insulin receptor; Leptin Signaling in obesity	1	2	miR-106a-5p, miR-301a-3p, miR-145-5p

Supplemental Figure 1 Absolute cycle thresholds (Cts) and normalized microRNA (miRNA) density in plasma and plasma extracellular vesicles (EVs).

Cts and normalized miRNA density in plasma

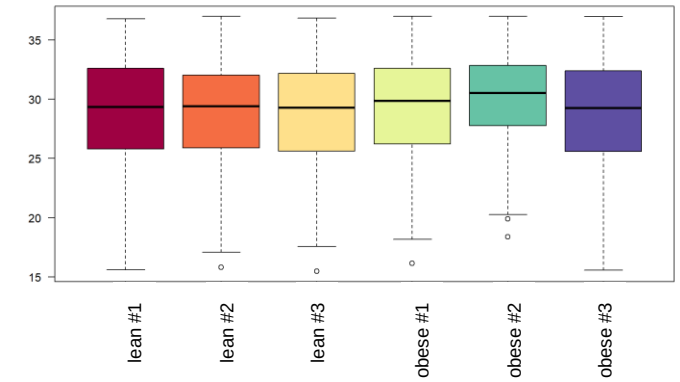

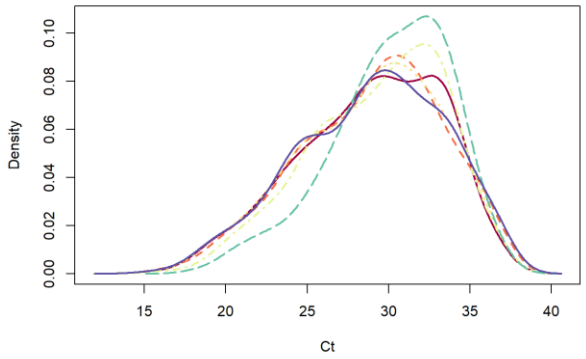

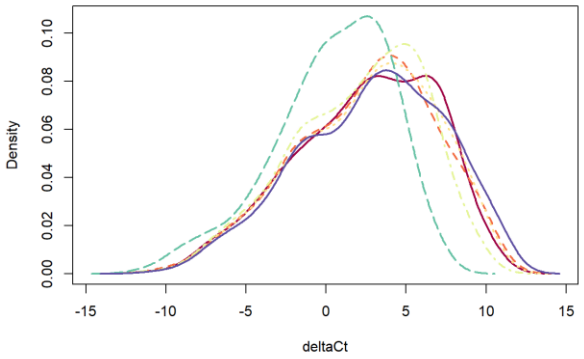

Cts and normalized miRNA density in plasma EVs

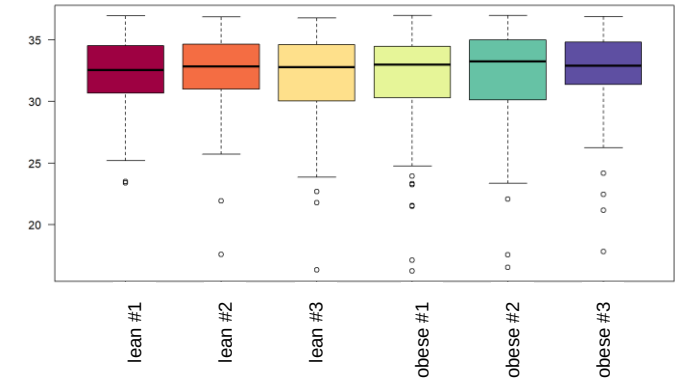

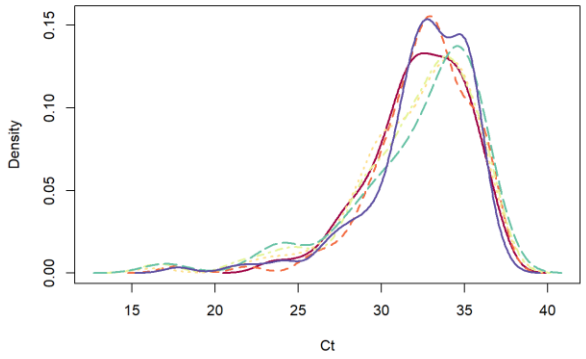

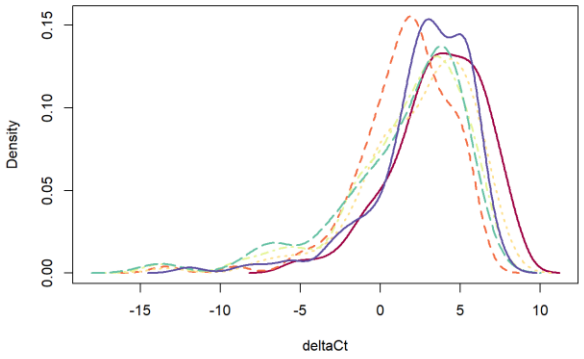

Supplemental Figure 2 A. Detection patterns and **B.** cluster analysis of miRNA profiles assessed in pooled plasma EVs and pooled paired-plasma samples. “Undetermined” stands for Ct values ≥ 37.

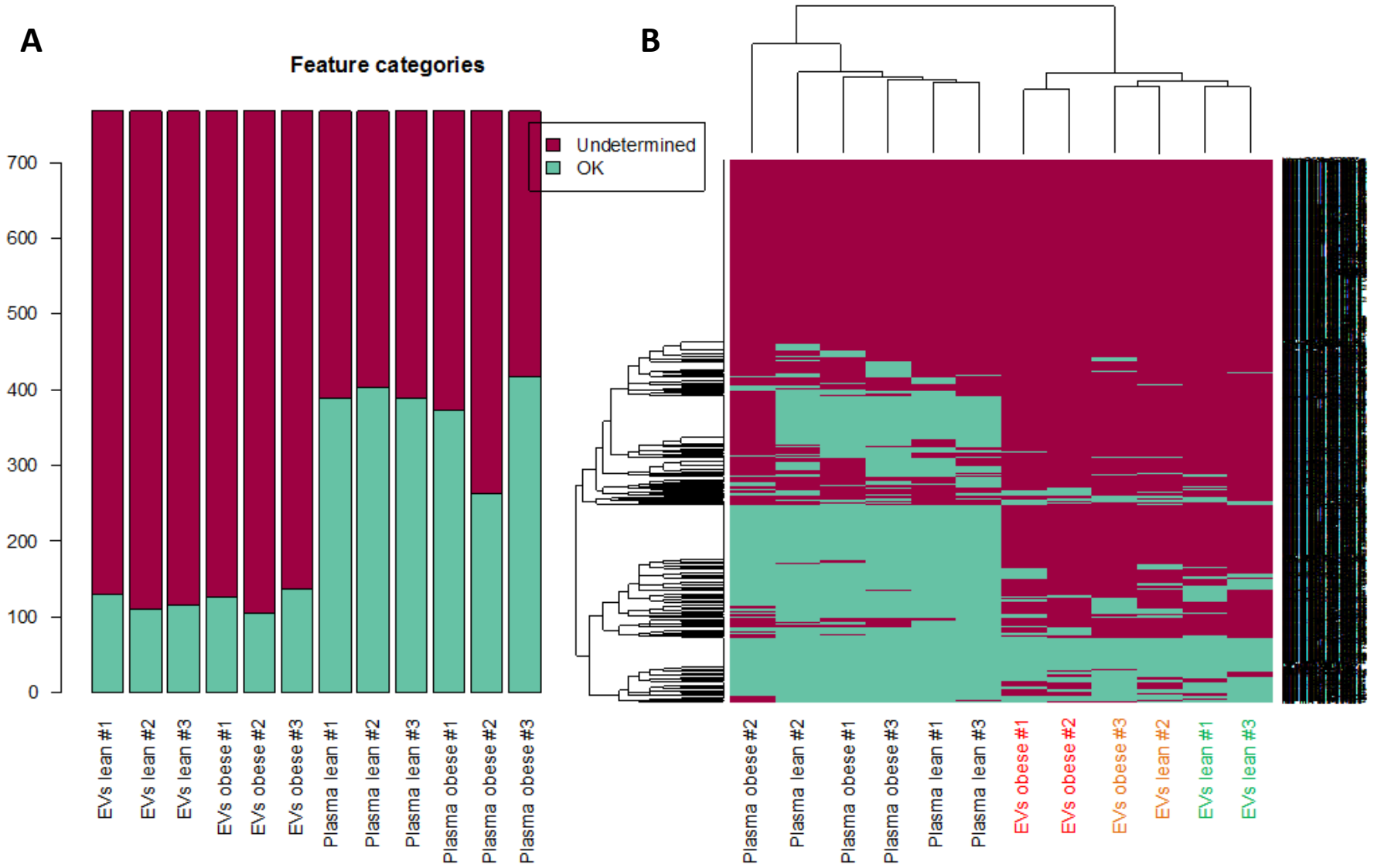

Supplemental Figure 3 Venn diagram of miRNAs with Ct values < 35 in all samples/group and multiple sequence alignment analysis comparing the miRNAs found in lean/obese plasma and obese EVs (2), lean/obese plasma and lean EVs (9), and lean/obese and lean/obese EVs (47 miRNAs).

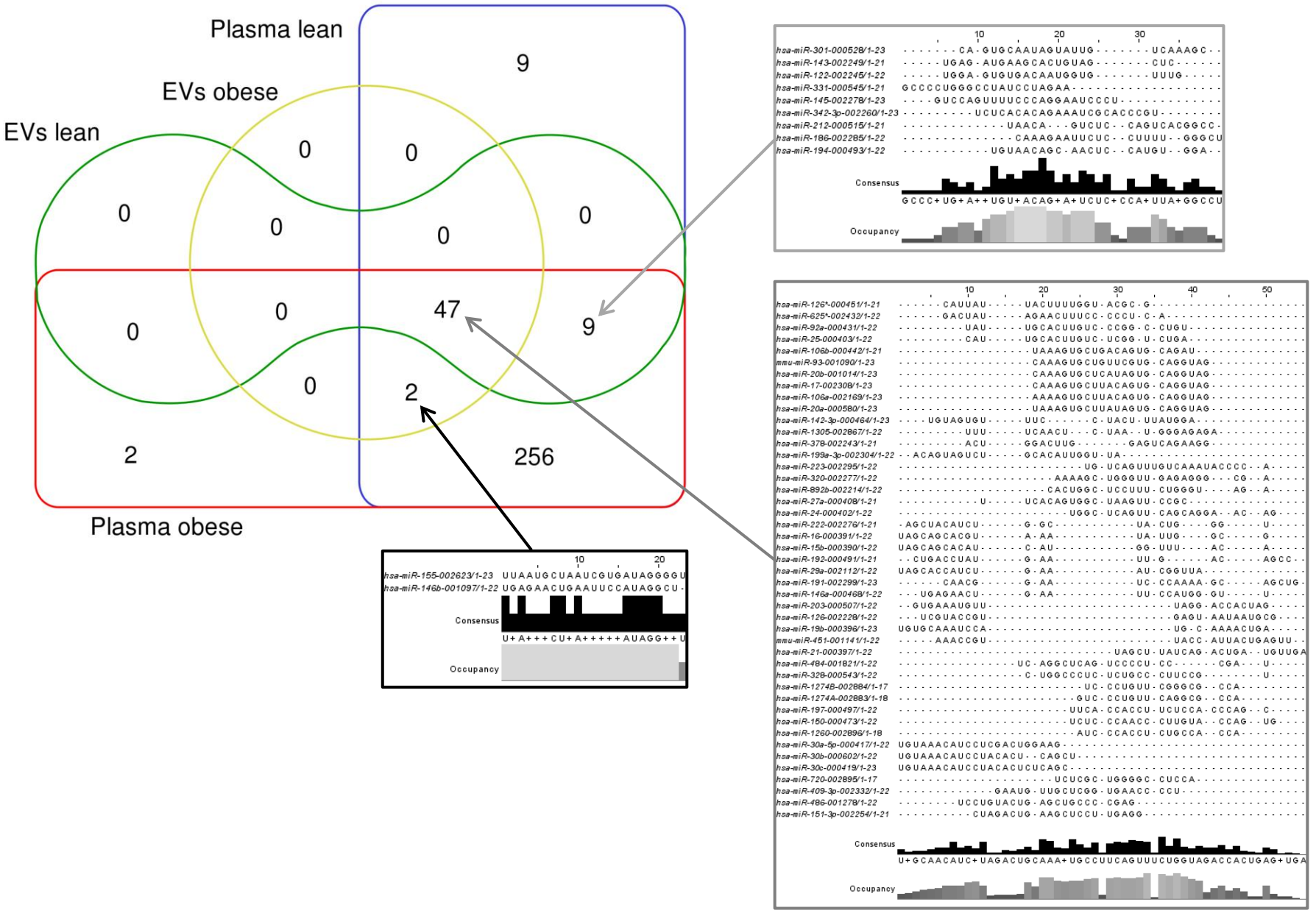

Supplemental Figure 4 Estimated tissue origin of miRNAs found in plasma EVs grouped according to the shared family.

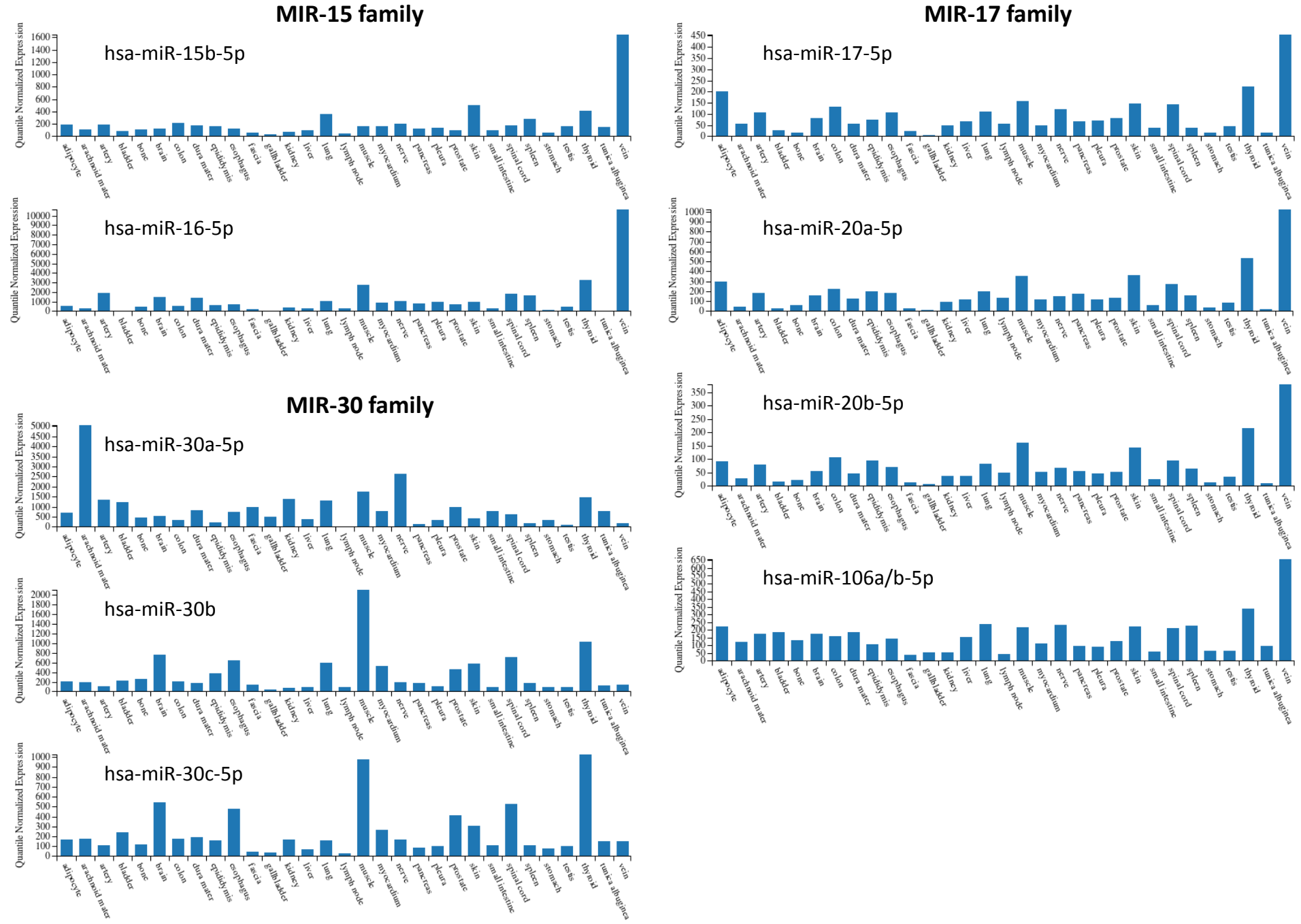

Supplemental Figure 5 Normalized miRNA clustering and heatmaps in plasma and plasma EVs.

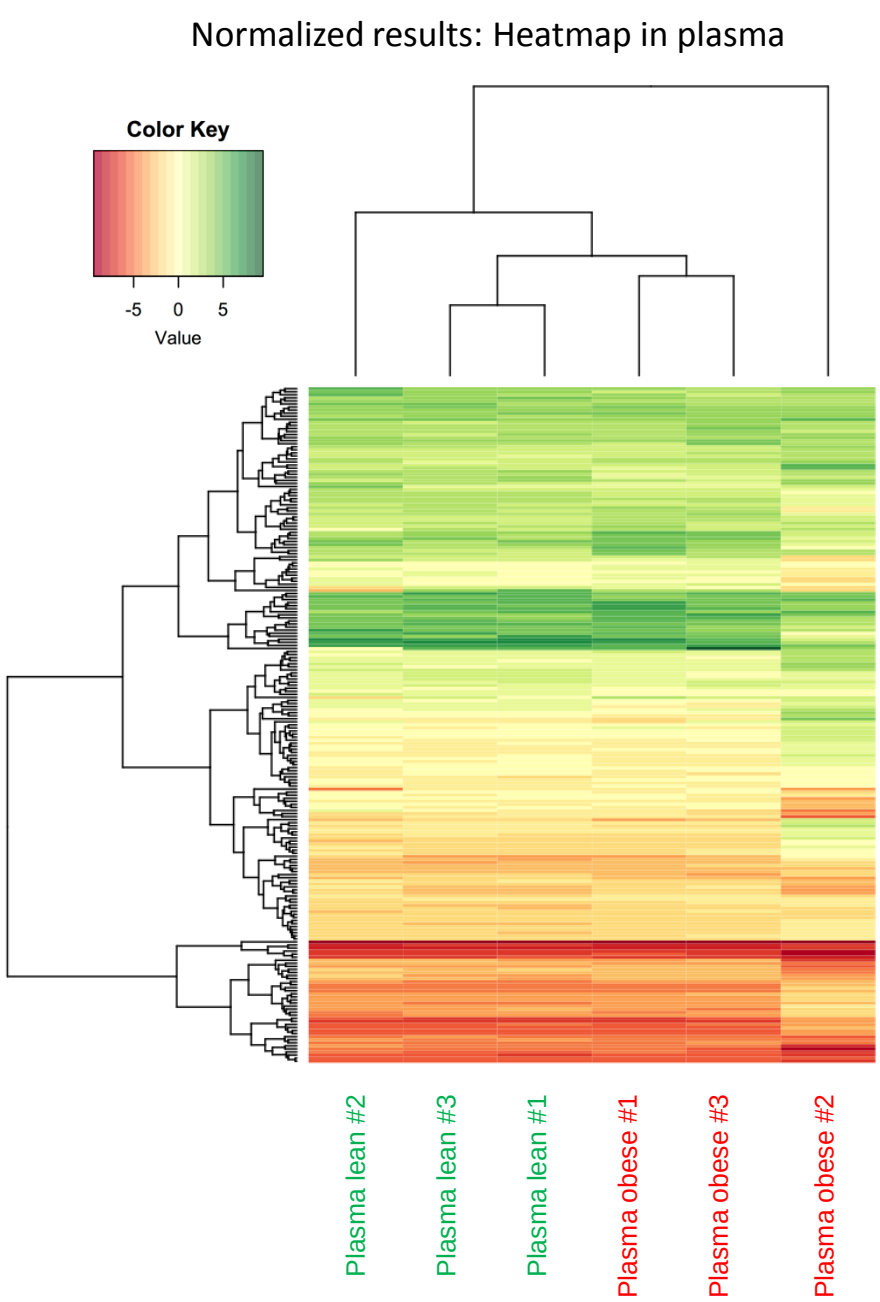

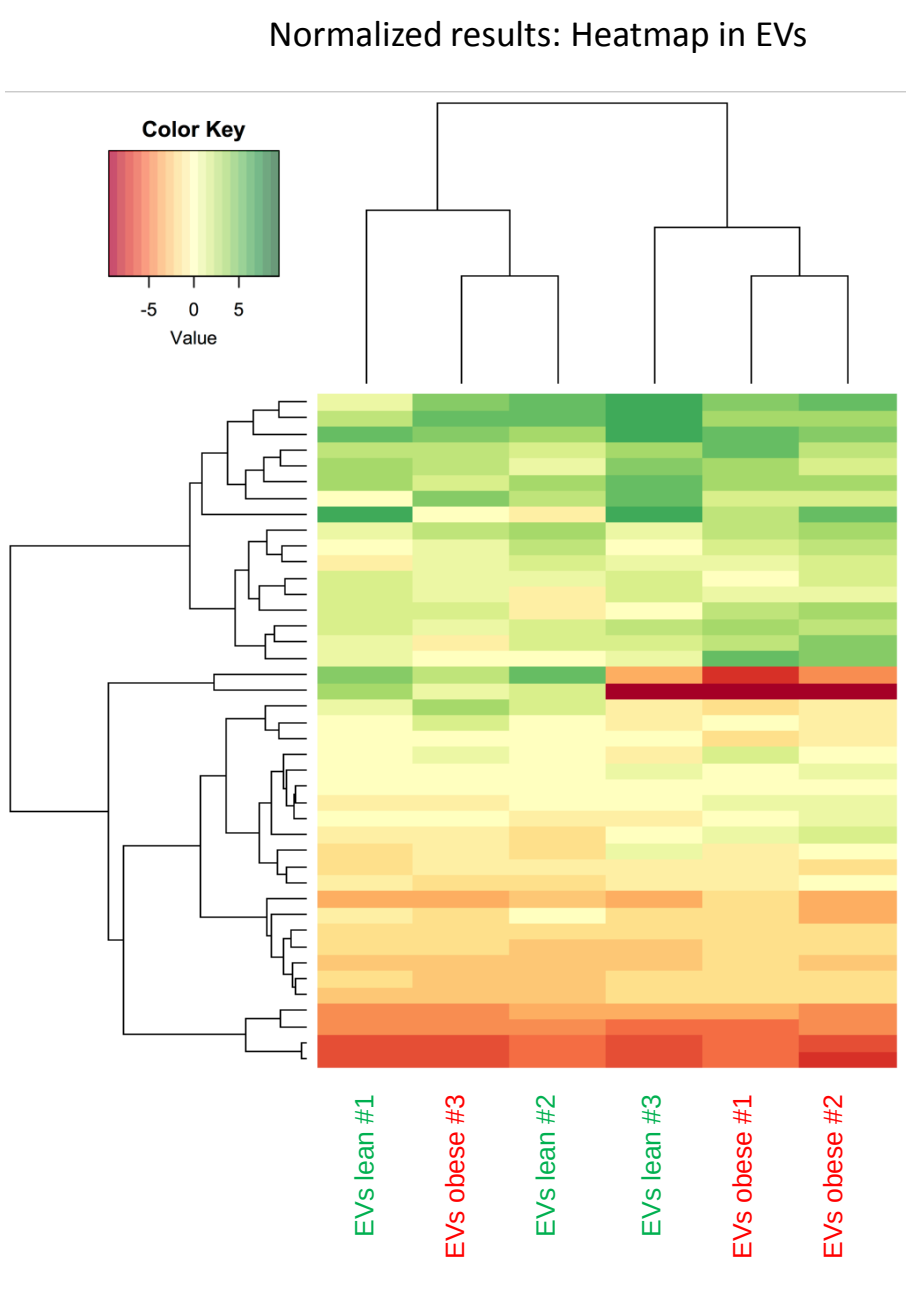

***ICMJE Conflict of Interest**

Please wait...

If this message is not eventually replaced by the proper contents of the document, your PDF viewer may not be able to display this type of document.

You can upgrade to the latest version of Adobe Reader for Windows®, Mac, or Linux® by visiting http://www.adobe.com/go/reader_download.

For more assistance with Adobe Reader visit http://www.adobe.com/go/acrreader.

***ICMJE Conflict of Interest**

Please wait...

If this message is not eventually replaced by the proper contents of the document, your PDF viewer may not be able to display this type of document.

You can upgrade to the latest version of Adobe Reader for Windows®, Mac, or Linux® by visiting http://www.adobe.com/go/reader_download.

For more assistance with Adobe Reader visit http://www.adobe.com/go/acrreader.

***ICMJE Conflict of Interest**

Please wait...

If this message is not eventually replaced by the proper contents of the document, your PDF viewer may not be able to display this type of document.

You can upgrade to the latest version of Adobe Reader for Windows®, Mac, or Linux® by visiting http://www.adobe.com/go/reader_download.

For more assistance with Adobe Reader visit http://www.adobe.com/go/acrreader.

***ICMJE Conflict of Interest**

Please wait...

If this message is not eventually replaced by the proper contents of the document, your PDF viewer may not be able to display this type of document.

You can upgrade to the latest version of Adobe Reader for Windows®, Mac, or Linux® by visiting http://www.adobe.com/go/reader_download.

For more assistance with Adobe Reader visit http://www.adobe.com/go/acrreader.

***ICMJE Conflict of Interest**

Please wait...

If this message is not eventually replaced by the proper contents of the document, your PDF viewer may not be able to display this type of document.

You can upgrade to the latest version of Adobe Reader for Windows®, Mac, or Linux® by visiting http://www.adobe.com/go/reader_download.

For more assistance with Adobe Reader visit http://www.adobe.com/go/acrreader.

***ICMJE Conflict of Interest**

Please wait...

If this message is not eventually replaced by the proper contents of the document, your PDF viewer may not be able to display this type of document.

You can upgrade to the latest version of Adobe Reader for Windows®, Mac, or Linux® by visiting http://www.adobe.com/go/reader_download.

For more assistance with Adobe Reader visit http://www.adobe.com/go/acrreader.

***ICMJE Conflict of Interest**

Please wait...

If this message is not eventually replaced by the proper contents of the document, your PDF viewer may not be able to display this type of document.

You can upgrade to the latest version of Adobe Reader for Windows®, Mac, or Linux® by visiting http://www.adobe.com/go/reader_download.

For more assistance with Adobe Reader visit http://www.adobe.com/go/acrreader.

***ICMJE Conflict of Interest**

Please wait...

If this message is not eventually replaced by the proper contents of the document, your PDF viewer may not be able to display this type of document.

You can upgrade to the latest version of Adobe Reader for Windows®, Mac, or Linux® by visiting http://www.adobe.com/go/reader_download.

For more assistance with Adobe Reader visit http://www.adobe.com/go/acrreader.

***ICMJE Conflict of Interest**

Please wait...

If this message is not eventually replaced by the proper contents of the document, your PDF viewer may not be able to display this type of document.

You can upgrade to the latest version of Adobe Reader for Windows®, Mac, or Linux® by visiting http://www.adobe.com/go/reader_download.

For more assistance with Adobe Reader visit http://www.adobe.com/go/acrreader.

***ICMJE Conflict of Interest**

Please wait...

If this message is not eventually replaced by the proper contents of the document, your PDF viewer may not be able to display this type of document.

You can upgrade to the latest version of Adobe Reader for Windows®, Mac, or Linux® by visiting http://www.adobe.com/go/reader_download.

For more assistance with Adobe Reader visit http://www.adobe.com/go/acrreader.

***ICMJE Conflict of Interest**

Please wait...

If this message is not eventually replaced by the proper contents of the document, your PDF viewer may not be able to display this type of document.

You can upgrade to the latest version of Adobe Reader for Windows®, Mac, or Linux® by visiting http://www.adobe.com/go/reader_download.

For more assistance with Adobe Reader visit http://www.adobe.com/go/acrreader.